

RSC Advances



This is an *Accepted Manuscript*, which has been through the Royal Society of Chemistry peer review process and has been accepted for publication.

Accepted Manuscripts are published online shortly after acceptance, before technical editing, formatting and proof reading. Using this free service, authors can make their results available to the community, in citable form, before we publish the edited article. This *Accepted Manuscript* will be replaced by the edited, formatted and paginated article as soon as this is available.

You can find more information about *Accepted Manuscripts* in the [Information for Authors](#).

Please note that technical editing may introduce minor changes to the text and/or graphics, which may alter content. The journal's standard [Terms & Conditions](#) and the [Ethical guidelines](#) still apply. In no event shall the Royal Society of Chemistry be held responsible for any errors or omissions in this *Accepted Manuscript* or any consequences arising from the use of any information it contains.

Synthesis of a novel pH responsive phyllosilicate loaded polymeric hydrogel based on poly (acrylic acid-co-N-vinylpyrrolidone) and polyethylene glycol for drug delivery: Modelling and kinetics study for sustained release of antibiotic drug

Sayan Ganguly, Narayan Ch. Das*

Rubber Technology Centre, Indian Institute of Technology, Kharagpur 721302, India

Abstract

In this study, we developed the novel pH-sensitive composite interpenetrating polymeric network (IPN) hydrogel based on polyethylene glycol (PEG), poly(acrylic acid-co-N-vinylpyrrolidone) crosslinked with N,N-methylenebisacrylamide (MBA). These composite is used in the controlled release (CR) of cefadroxil, an antibiotic drug. A systematic method via in-situ polymerization in sodium aluminosilicate dispersion media is also performed in order to achieve much higher degree of swelling behaviour followed by sufficient gel strength in the simulated pH atmosphere. The resulting hydrogel imprinted was characterized by Fourier transform infrared spectroscopy (FTIR) to confirm the copolymer formation and cross linking reaction and scanning electron microscopy (SEM) to understand the surface morphology. Differential thermal analysis - thermo gravimetric analysis (DTA-TGA) and X-ray diffraction (XRD) were also used for investigating deviations from crystallinity and swelling experiments. In vitro release of the drug loaded hydrogel results performed in acidic and basic media affected the drug release characteristics. Release data have been analysed using an empirical equation to understand about the transport of drug containing solution through the polymeric matrices. The wt% of PEG, MBA, initiator, total monomer concentration, pH of the medium was found to strongly influence the drug release behaviour of the gels. Impression of drug loading on encapsulation efficiency was also investigated. The release rate of the drug was much faster at pH of 7.8 than at pH 1.7. Modelling and kinetics of sustained release of antibiotic was reported.

Key words: polyethylene glycol, poly(acrylic acid-co-N-vinylpyrrolidone), composite hydrogel, synthesis, characterization, drug release

*Corresponding Author: ncdas@rtc.iit.kgp.ernet.in (N. C. Das)

Introduction

Hydrogels are one of the forth coming families of polymer-based sustained-release drug delivery systems. Besides displaying swelling-controlled drug release, hydrogels also show stimuli responsive deformational attitude in their morphological network and the drug release. Because of large variations in physiological pH at various body sites in normal as well as pathological simulated conditions, pH-responsive polymeric networks have been extensively studied^{1,2}. PEG hydrogels have been widely explored as water-soluble biocompatible, non-toxic, non-immunogenic and level of bioadhesive polymer for numerous biomedical and pharmaceutical applications³. A wide range of material properties can be obtained by tuning of the PEG and the crosslinker compositions. So, hydrogels based on PEG with different cross-linked structure, create unique opportunities for controlling pH sensitive drug carriers, designing tissue engineering scaffolds. For free radical solution polymerization, total monomer concentration in water should be at least 15-20 wt% while it is difficult to make an aqueous solution. In the present work PEG was incorporated in poly(acrylic acid-co-vinylpyrrolidone) based gel by in situ incorporation during simultaneous crosslink between acrylic acid and MBA or N-vinylpyrrolidone and MBA in water medium. Acrylic acid and N-vinylpyrrolidone both are water soluble monomer and chosen since its copolymer is a pH responsive polyelectrolyte which is immensely reliable for drug delivery to specific sites of gastrointestinal tract⁴. Hydrogels based on N-vinylpyrrolidone (NVP) as a co-monomer have been applied successfully as local dressings on wound treatments, such as burns, skin's ulceration and postoperative dressings⁵. In recent years, polymer/layered silicate (PLS) nanocomposites have attracted great interest, both in industry and in academia, because they often exhibit remarkable improvement in materials desired properties when compared with

virgin polymer or conventional micro, nano and their composites⁶⁻⁹. Although the intercalation chemistry of polymers when mixed with appropriately modified layered silicate and synthetic layered silicates has long been known in this composite hydrogel development context.¹⁰⁻¹²

In this work, our aim is to develop a hydrogel, which has some reasonable biocompatibility and the responsiveness to external surroundings stimuli. So we used N-vinylpyrrolidone (NVP) as an essential material of gel-forming. Synthesis of hydrogel follows two steps. In step one, we synthesized crosslinked gel bead through the chemical reaction. In the second step we synthesized the semi-IPN composite hydrogel based on hydrophilic clay reinforcement stabilized through the interaction among the carboxylic acid groups, micropores and the interstices between the two networks. The copolymer formation and crosslinking reaction of the hydrogel was investigated by FTIR and swelling experiment. Morphology and crystallinity of the hydrogel was investigated by SEM, DTA-TGA and XRD. In vitro release of the drug loaded hydrogel results performed in acidic and basic media affected the drug release characteristics. Release data have been analysed using an empirical equation to understand about the transport of drug containing solution through the polymeric matrices. The wt% of PEG, MBA, initiator, total monomer concentration, pH of the medium was found to strongly influence the drug release behaviour of the gels. The modelling and kinetics for the sustained release of antibiotic drug has been studied.

2. Experimental methods

2.1. Materials

Polyethylene glycol 4000 (PEG, Merck) was used without any further purification. The analytical grade co-monomer crosslinking agent, N, N'-methylene bisacrylamide(MBA, from Merck) and the redox pair of initiators ammonium persulfate (APS, from Fluka) and sodium

metabisulfite were used without any further purification. The monomer acrylic acid (AA, Merck) and N-vinylpyrrolidone (NVP, Merck Schuchardt OHG, Germany) were used after vacuum distillation. Hydrophilic sodium montmorillonite aluminosilicate filler was used after drying at 110⁰C for 2 hours in oven (rich nano size 30-90 nm, aspect ratio 300-500, mineral's thickness 1nm, cation exchange capacity 120 m_{eq}/100 g). The specification of this filler is reported elsewhere¹³; Bentonite filler was supplied by Amrfeopte. Ltd., Kolkata. The drug cefadroxil was provided by Aristo Pharmaceuticals Pvt. Ltd., Solan, U.P.

2.2. Methods

2.2.1. Synthesis of composite hydrogel by in situ filler incorporation

At first poly(acrylic acid-co-vinyl pyrrolidone) gels were prepared at varied initiator, total monomer concentration, crosslinking agent, MBA concentration and PEG concentration in a three necked reactor placed on a constant temperature bath and fitted with a stirrer, a thermometer pocket and a condenser at 60⁰C. For preparing composite gel varied concentrations, i.e., 1.0, 2.0, 3.0 and 4.0wt% of PEG was made in deionised water. The required amount of PEG solution and monomers (AA: NVP=10:1) were then poured into the reactor. Temperature was maintained at 60⁰C and aqueous solution of initiators was added to the reactor followed by the addition of MBA (crosslinker). After polymerization the reaction mixture was cooled to ambient temperature. Hydrophilic aluminosilicate (zeolyte) filler was first dispersed in water well for one an hour followed by addition of monomers and stirring for another half hour. Then, the polymerization with in situ mixing of filler with these monomers was carried out in a similar way as in the case of polymerization for the unfilled (without any filler) gel. In another terms of experiment AA is partially neutralised with NaOH and then this monomer is copolymerized with NVP in presence of PEG according to the

previous method stated above. Hydrophilic clay (nanobentonite) is also used here to optimise the swelling as well as gel strength. Hydrogel obtained was disintegrated into small blocks and then immersed into 1:3 v/v ethanol-water solution for 48 hours to remove water soluble oligomer, unreacted monomers and the initiator fractions.

2.2.2. Yield, Gel and Sol content of the hydrogel

The hydrogels as prepared above were first dried to a constant weight (W_c) in a vacuum oven and then it was taken in water and kept for a week with occasional shaking to remove the water soluble part from the hydrogel. The water insoluble gel sample was further dried (xerogel) in vacuum oven to a constant weight (W_d). Yield, gel and sol% was obtained as

$$\text{Yield\%} = \frac{W_c}{W_i} \times 100 \quad (1)$$

$$\text{Gel\%} = \frac{W_d}{W_c} \times 100 \quad (2) \quad \text{Sol\%} = 100 - \text{Gel\%} \quad (2a)$$

Where W_i is total weight of monomers (AA, NVP and MBA) and PEG used for synthesis of gel.

2.3. Characterization of the hydrogels

2.3.1. Swelling experiment

The equilibrium swelling ratio (ESR) was evaluated gravimetrically. For studying dynamic swelling properties the gel samples were immersed in double distilled water at ambient temperature and mass of the swollen gel sample (m_t) was taken at different time intervals until there was no change of mass with time. The equilibrium swelling ratio (ESR) of the hydrogels was determined by using the following Eq. 3

$$\text{ESR} = \frac{W_s - W_d}{W_d} \quad (3)$$

Where W_s and W_d are the weights of swollen and dried hydrogels respectively.

At swelling equilibrium point, $W_s = W_e$. Thus, Equilibrium swelling ratio (ESR) was obtained from Eq. (3) by replacing W_s with W_e . The buffer solutions of varied pH was prepared by dissolving phosphoric acid, potassium phosphate (KH_2PO_4), potassium hydrogen phosphate (K_2HPO_4) and sodium hydroxide in double distilled water. Ionic strengths of the buffer solutions were adjusted to 0.1 molar with sodium chloride solution. The pH values were determined by a pH meter. Swelling of the hydrogel samples were also carried out at different ionic strengths in presence of NaCl , CaCl_2 and AlCl_3 .

2.3.2 Factorial Design for swelling study

Customarily, the pharmaceutical formulations which are developed by changing the single variable at a time is soundly upgraded by factorial design followed by interaction method¹⁴. In this factorial design, the influences of all experimental variables, either independent (total monomer concentration, PEG concentration, crosslinker concentration, initiation concentration) or dependent variable (swell ration) having their subtle interaction effects on their responses are investigated with 4th order interaction effect on the responses.

2.3.3. Fourier Transform Infrared (FTIR) Spectroscopy

FTIR spectra of the drug free and drug loaded hydrogel samples were performed by a FTIR spectrometer (Perkin Elmer, model-Spectrum-2, Singapore) using KBr pellet made by mixing KBr with fine powder of the drug free and drug loaded gel samples. (10:1 mass ratio of KBr to polymer, for only drug sample 50:1 ratio of KBr to drug was used).

2.3.4. Thermal Analysis

Differential thermal analysis (DTA) and thermogravimetric analysis (TGA) of the hydrogel samples were carried out in a Perkin Elmer instrument in nitrogen atmosphere at the scanning rate of 10°C /min in the temperature range of 25 to 600°C.

2.3.5. X-ray diffraction (XRD)

Wide angle XRD profile of the gel samples were studied at room temperature in a diffractometer (model: X'Pert PRO, made by PANalytical B.V., The Netherlands) using Ni-filtered Cu K α radiation ($\lambda=1.5418$ Å) and a scanning rate of 0.005 deg (2 θ)/s). The angle of diffraction was varied from 2-72 degree.

2.3.6. Scanning electron microscopic (SEM) studies

The morphology of the gold coated Semi-IPN gels were observed by using SEM (Scanning electron Microscope, model no. S3400N, VPSEM, Type-II, made by Hitachi, Japan) with the accelerating voltage set to 15 kV.

2.3.7. Point zero charge (PZC) analysis

For PZC analysis small amount of hydrogel sample (~50 mg) was taken in a 100 mL conical flask containing 0.1 normal potassium nitrate solutions. The pH of the solution (pH_i) was adjusted between 2 and 12 by adding either 0.1N nitric acid or sodium hydroxide¹⁵. The solution containing the gel sample was then kept for 48 hours to reach equilibrium with occasional shaking. The pH of the supernatant liquid was measured (pH_f). The difference between this initial and final pH ($\Delta\text{pH} = \text{pH}_i - \text{pH}_f$) was plotted against pH_i and the point of intersection of the curve at $\Delta\text{pH} = 0$ gives the value of PZC for the hydrogel.

2.3.8. Study of pH-reversibility

The buffer solutions with various pH values were set up by combining KH_2PO_4 , K_2HPO_4 , H_3PO_4 , HCl and NaOH solution properly. The pH values were determined by a pH meter. The equilibrium water uptake in various pH solutions was determined by a method similar to that in distilled water. The pH reversibility of the hydrogel samples were investigated in terms of its swelling-deswelling oscillatory behavior in pH buffer solution of phosphate between pH 7.8 and 1.7. The sequential time interval is 30 min for each cycle.¹⁶

2.4. Evaluation of network parameter

The gel network is usually characterized in terms of average molecular weight between crosslinks, M_c and mesh size, ζ , measured by neutron scattering or quasi-elastic light scattering¹⁷. M_c is obtained from the following equation based on network theory of Flory and Rehner¹⁸.

$$M_c = - \frac{V_s \rho_p (\phi_p^{\frac{1}{3}} - \frac{\phi_p}{2})}{\ln(1 - \phi_p) + \phi_p + \chi \phi_p^2} \quad (4)$$

The molar volume of water, V_s at experimental temperature (25⁰C) was calculated (18.18 cm^3/mole) from its density (0.98 g/cm^3) and molecular weight (18 g/mole), the density of hydrogel sample, ρ_p was calculated from its mass and volume. The volume of the polymer sample was measured by the method reported elsewhere¹⁹. For equilibrium swelling of m_w g water/g dry hydrogel sample, polymer volume fraction in swollen gel under equilibrium, ϕ_p will be

$$\phi_p = \left(1 + \frac{\rho_p}{\rho_i} m_w\right)^{-1} \quad (4a)$$

Where, ρ_p and ρ_i are density of polymer and solvent (water), respectively. The polymer–solvent interaction parameter, χ between water and polymer hydrogel is obtained using the following Equation [20].

$$\chi = \frac{V_p}{3} + 0.5 \quad (4b)$$

Crosslink density (ρ_c) of a hydrogel is obtained as

$$\rho_c = \frac{\rho_p N_A}{M_c} \quad (4c)$$

N_A is Avagadro's number ($6.023 \times 10^{23}/\text{mol}$). The mesh size (ζ in Å) of the swollen polymeric network is calculated from the following Eq.²¹

$$\zeta = [C_n \left(\frac{2M_c}{M_r}\right)]^{\frac{1}{2}} I \phi_p^{\frac{1}{3}} \quad (4d)$$

The Flory's characteristic ratio, C_n was taken from literature and C–C bond length; 'I' was assumed as 1.54 \AA^2 . M_r , the molecular weight of repeat unit was calculated as the weight average of the repeat unit of PEG ($M_r = 62$) and poly (acrylic acid-co-N-vinylpyrrolidone) ($M_r = 184$).

2.5. Study of drug loading and entrapment efficiency of the hydrogel

Drug loading and entrapment efficiency of the hydrogel samples were carried out by similar experiments as reported elsewhere. For drug loading the hydrogel samples of specified weight (W_i) were first swollen in 100 mL water-ethanol mixture (20 % ethanol (v/v) of constant pH and ionic strength (pH 1.7 simulating gastric fluid and 7.8 simulating intestine fluid and ionic strength 0.1 mol/L) and containing specified amount (W_o) of cefadroxil drug. After 72 h of swelling, the drug loaded wet hydrogel samples were carefully taken out from the solution and

washed with the same solution to remove free drug from the sample. Drug loading (DL) and entrapment efficiency of the hydrogel sample was determined as

$$\text{DL (mg/g hydrogel sample)} = \frac{W_d - W_i}{W_i} \quad (5)$$

$$\text{Entrapment efficiency (\%)} = \frac{W_d - W_i}{W_o} \times 100 \quad (5a)$$

Where W_d is weight of the drug loaded dry hydrogel sample.

2.6. In vitro drug release studies

In vitro release of the drugs from the hydrogel samples was carried out at $35 \pm 0.5^\circ\text{C}$ using Indian Pharmacopoeia (IP) Dissolution Test Apparatus Type 2 (paddle method) at a rotation speed of 50 rpm in 100 mL of buffer (pH 1.7 & 7.8) for 7-9 hours. The drug loaded wet samples obtained from drug loading test were first dried overnight at ambient condition followed by drying in a vacuum oven at 50°C for another three days. The drug loaded dry samples were then immersed in buffer solution of same composition. At several time intervals 5mL of the solution containing released drug was withdrawn and at the same time 5 mL fresh solution was added to keep the solution volume constant. The concentration of drug in the withdrawn solution was analyzed by UV-Vis spectrophotometer (Lamda 25, Perkin Elmer, Singapur) at λ_{max} of 230 nm for cefadroxil using a calibration curve constructed from a series of the drug solutions of known concentrations. All release experiments were carried out in triplicates and the average values were considered. The drug release % was obtained as

$$\text{Drug release\%} = \frac{W_{\text{drug}} - W_{\text{release}}}{W_{\text{release}}} \times 100 \quad (5b)$$

Where W_{drug} is mass of drug loaded gel sample and W_{release} is mass of drug released in the solution.

3. Results and discussion

3.1 Synthesis of composite hydrogels

In the present work acrylic acid, N-vinyl pyrrolidone (NVP) and MBA undergoes free radical crosslink copolymerization in water in presence of PEG. During free radical polymerization three acrylic monomers copolymerize with three vinyl ($\text{CH}_2=\text{CH}-$) functional groups of one MBA monomer and thus a three dimensional network of crosslink copolymer gel is formed as shown in the Fig.1a followed by scheme 1. Further, some of the (-OH) groups of PEG reacts with carboxylic (-COOH) functional groups of acrylic acid to form polyester type complex (-COO-) ²³. Accordingly, a stable composite hydrogel is formed where the dispersed phase, i.e. PEG is chemically and covalently bonded to the continuous acrylic copolymer phase. The formation of the composite gel is shown in scheme 1 while the structure of the two drug molecules viz. cefadroxil is shown in Fig. 1b. The copolymer in the semi-IPN type gel is also confirmed by NMR spectra elsewhere.^{4,24} A peak was reported at 81.79 ppm in the gel spectrum, which is a signal of quaternary carbon atom (4^0 Carbon) groups in the freshly- built cross bond. The change is consistent with the fact that the N-CH attached group partially altered into quaternary carbon atom (4^0 Carbon) groups in the backbone chain. The carbonyl carbon peak at 215.40 ppm vanished after crosslinking.

3.1.1. Effect of reaction variables on gel content and gel time of the hydrogels

The effect of initiator (I), monomer (AA and NVP), crosslinker (MBA) and polyethylene glycol (PEG) on gel content (%), yield (%) and gel time of the hydrogels are shown in Fig.1c. For studying effect of single parameter, other parameters were kept constant viz. when

concentration of initiator was varied as 0.5, 0.8, 1.0 and 1.5wt% (of total monomer weight) , the amount of crosslinking agent and monomer were kept constant at 1 wt% and 20wt%, respectively. Fig.1c depicts that the increase in initiator concentration from 0.5 to 1.5wt% yield or gel% decrease gel time. In fact, the rate of polymerization increases at higher initiator concentration resulting in polymer gel of shorter chain length (lower molecular weight). Thus, gelling occurs at an early stage of polymerization resulting in shorter gel time and less gel%.²⁵ At very low initiator concentration viz, 0.5 wt% initiator, the generation of free radicals from initiator is too low. Thus, yield or gel% is observed to increase from 0.5 to 1.5 wt% initiator in polymerization mixtures. The network (gel) in the polymer is formed at a much faster rate in presence of increased amount of crosslinker, i.e., MBA. Similarly, the yield or gel % also increases with concentration of crosslinker due to increase in rate of polymerization in presence of increased amount of reactant (crosslinker). However, at 2.5wt% crosslinker, yield or gel% decreases because of formation of network at an early stage of polymerization¹⁵. The effect of total monomer concentration in reaction medium on synthesis of gel is also shown in Fig.1c. With increase in monomer (acrylic acid, vinyl pyrrolidone) concentration in water yield or gel% is observed to increase which may be attributed to generation of large number of active primary radicals at higher monomer concentration in water²⁵. It is also observed that the gel time decreases with increase in monomer concentration in water. This is because gelling occurs early due to increased reaction rate at higher monomer concentration. From Fig.1c it is also observed that gel time, yield% and gel% increases with increase in wt% of PEG in the hydrogel. At higher concentration of PEG, the solution viscosity increases and the same amount of MBA and monomers take longer time to gel in the viscous medium. However, PEG also takes part in the polymerization reaction by forming macro radicals and hence yields or

gel% is observed to increase with increase in amount of PEG in the hydrogel²⁶. At 4wt% PEG viscosities of the reaction medium increases significantly and hence extent of polymerization reaction decreases with decrease in yield or gel%.

3.1.2. Factorial design

Effects of individual variables (X_1 , X_2 , X_3 and X_4) and their interactions between the four variables in the factorial design of swelling experiments was computed using the sign table (Table 2) for the counterpoint constants for 2^4 design as offered by Montgomery (1997)²⁷. After performing the fourth order interaction model analysis from these contrasts, we have reckoned the 15 factorial effects. The correlation between effective experimental variables (X_1 , X_2 , X_3 and X_4) and the dependant variable (swell ratio, SR) was evaluated by the multiple linear regressions. The method of fourth order interaction model analysis was used to compute regression coefficients and the following polynomial equation was derived:²⁸

$$y = 16.699813 + 4.0108125 X_1 + 1.992938 X_2 + 1.4666875 X_3 + 5.5808125 X_4 + 2.046938 X_1X_2 + 0.3776875 X_1X_3 - 2.3306875 X_1X_4 - 0.93944 X_2X_3 - 2.25106 X_2X_4 - 1.1343125 X_3X_4 - 1.0854375 X_1X_2X_3 - 1.3995625 X_1X_2X_4 - 0.645438 X_2X_3X_4 - 1.4258125 X_1X_3X_4 + 3.986063.$$

Here, the coded variables X_1 , X_2 , X_3 , X_4 and y represent the variables PEG content, crosslinker concentration, initiator concentration, total monomer concentration and swell ratio respectively.

3.1.3 Effect of filler incorporation on swelling

Incorporation of hydrophilic phyllosilicate into the polymer gel vehemently affects the water uptake percentage as well as its equilibrium swelling ratio (ESR)²⁹. The composite meshing type network consisting with hydrophilic filler evidences higher water uptake in comparison

to unfilled hydrogel i.e. filler enhances the hydrophilicity of the gel. In contrast it is quite noticeable that beyond 4% filler loading the filler particles establishes another network prioritises over the hydrophilicity effect in swelling behavior as a result the swelling ratio became quite decreasing³⁰. The functional groups of polymer as well as hydrophilic filler participates in water absorption and the network structure of the gel filled with hydrophilic fillers takes much shorter time to reach saturation.

3.2. Characterisation of the hydrogels

3.2.1. FTIR spectra

In Fig. 2, for PEG a strong but broad absorption band appearing at 3442 cm^{-1} indicates its O-H and C-OH stretching while the absorption band at 2885 cm^{-1} is due to its CH_2 stretching vibration. The absorption band at 1342 cm^{-1} stands for its $-\text{CH}_2$ wagging vibration. Another characteristic absorption band of PEG at 1957 cm^{-1} is ascribed to its crystalline state. Similarly, the absorption band at 1098 cm^{-1} is due to C-O-C stretching and the absorption peak at 840 cm^{-1} corresponds to the vibration of its $-\text{CH}_2-\text{CH}_2-\text{O}$ group³¹. The 2892 cm^{-1} peak of PEG due to its CH_2 stretching is observed to shift to 2880 cm^{-1} in the gel. Similarly, the 3384 cm^{-1} peak of PEG due to its O-H and C-OH stretching is observed at 3317 cm^{-1} in gel sample, 3325 cm^{-1} in filler loaded gel. The Si-O vibration band at 1024 cm^{-1} of bentonite³² and C-O-C stretching of PEG at 1098 cm^{-1} is shifted to 1120 cm^{-1} in filler loaded gel. Similarly, the 519 cm^{-1} absorption peak corresponding to stretching vibration of Si-O-Al of bentonite³³ also possesses a strong shoulder in that region. All of these shifting and bifurcations signify strong electrostatic interaction among various functional groups of the hydrogels and the fillers³⁴. The FTIR spectra of poly (NVP-co-AA) after cross linking were carried out. The

results are shown in Fig. 2. It is already established that the carbonyl group of NVP segments exhibit a stretching vibration peak between 1650 and 1680 cm^{-1} and the group of carboxylic acid on the PAA chain exhibits a peak at approximate 1736 cm^{-1} from the literatures³⁵. When the carbonyl group frames intermolecular hydrogen bond, there is a negative shift exhibited in the FTIR spectrum. In this present work, the carbonyl group exhibits a peak at 1654 cm^{-1} for poly (NVP-co-AA) which shifted to but a peak at 1632 cm^{-1} for the polymeric gel, this negative shift from 1654 to 1632 cm^{-1} signify that a stronger inter-molecular interaction may takes place. Strong shoulder appearing at about 1734 cm^{-1} , which may be distinguished to stretching vibration of the carbonyl group of carboxylic acid on the PAA segments³⁶. Meanwhile, it is also manifested that a little shoulder appeared at about 1736 cm^{-1} corresponding to stretching vibration of carbonyl group of carboxylic acid group on the copolymer chain, which further exemplified that some intermolecular interaction due to hydrogen bond did occur and the complexation formed between carbonyl group acid segments of the acrylic acid³⁷⁻⁴⁰.

3.2.2. DTA and TGA

The DTA and TGA of the polymer samples are depicted in Fig.3. It is already established that virgin polyethylene glycol (PEG) shows an endothermic sharp melting peak at around 67°C and a weak exothermic inflection in base line at around 172°C due to oxidative degradation. PEG also shows exothermic peaks at 337°C and 372°C due to its decomposition and charcoal evolution⁴¹. PEG is observed to show a weight loss of around 10wt% up to a temperature of 275°C which is associated with loss of physically adsorbed water⁴². As the PEG is incorporated in the matrix of poly(acrylic acid-co-vinylpyrrolidone) it is shown that drug loaded gels, shows endothermic broad melting peaks in the temperature range of 200-280°C.

Similarly, the exothermic degradation peak of pure PEG at around 337 and 372°C is also shifted to a single exothermic peak at around 450-550°C in the copolymer gel. In case of pure drug the DTA peak are combined with the pure polymer peaks and generates new broad regions of melting. The drug loaded gel shows the crystallization peaks in between the pure drug and the pure copolymer gel. The drug loaded sample shows multiple degradation profiles which also again resultant of the drug and copolymer TGA behaviour.

3.2.3. X-ray Diffraction (XRD)

The XRD of pure PEG4000, montmorillonite clay and unfilled gel is shown in Fig. 4. The PEG is found out to show strong XRD peaks at two theta (2θ) of 19.8°, 23.8° and some weak peaks at 26.°, 36.6°, 40.5° and 46.2° as also reported elsewhere⁴³. Prominent intermolecular hydrogen bonding between –OH groups of PEG chain is responsible for its crystallinity and therefore rising of XRD peaks. Similar to PEG, the clay is also remarked to show respective diffraction peaks of its montmorillonite“001” planes at 2θ of 7.1°, 20.3°, 29°, 35.6° and 62.3° as also reported elsewhere⁴⁴.

3.2.4. Scanning Electron Microscopy (SEM)

Cross sectional morphology of poly (NVP-co-AA) hydrogel with moderate cross linking levels is shown in Fig.5. From this we can see that the hydrogel exhibits certain consistent and porous three-dimensional network structure. This may be owing to the effective cross linking bond triggered by free radical boosted MBA crosslinker. From these it is customary to say that the elastic nature and large free volume exhibited by poly(AA-co-NVP) hydrogel, which would be favorable for the movement of polymer chain segments and migration of charged particles in the interior of the hydrogel⁴⁵.

3.2.5. Point Zero Charge (PZC) analysis

The change of state of ionization of the functional groups of the hydrogels with solution pH is evaluated in terms of its point zero charge (PZC). The initial pH of a solution (pH_i) changes in presence of hydrogel. The difference between this final pH (pH_f) and initial pH (pH_i), i.e., $\text{pH}_i - \text{pH}_f$ is plotted against initial solution pH (pH_i) in Fig.6a. The pH of the solution (pH_{PZC}) at which $\text{pH}_i - \text{pH}_f$ is zero is called point zero charge. Thus, the hydrogel will remain neutral at solution $\text{pH} = \text{pH}_{\text{PZC}}$, positively charged at solution $\text{pH} < \text{pH}_{\text{PZC}}$ or negatively charged at solution $\text{pH} > \text{pH}_{\text{PZC}}$ ⁴⁶. From Fig.6a it is observed that PEG shows a pH_{PZC} of 9.98. It implies that carboxylic acid group will remain in protonated form (-COOH) at moderate pH (almost 3 for unfilled and 6 for filled gel). It is also observed that In fact, in presence of PEG negative charge of acrylic acid segments is reduced because of organization of 'polyion' complex⁴⁷. Thus, pH_{PZC} of IPN gel decreases. The full IPN shows slightly lower pH_{PZC} than semi-IPN which may be due to cross linking of PEG in the IPN hydrogels.

3.2.6. pH-sensitivity

Fig.6b depicted the dependence of water absorption for PEG/poly (acrylic acid-co-N-vinyl pyrrolidone) semi-IPN on pH of external buffer solution (0.10 mol/L). It can be clearly observed that the almost does not swell at pH 1.7, but it sharply swell as enhancing external pH values until a plateau was reached ($\text{pH} > 4$). The evident change of water absorption with altering the pH of external buffer solution con-firmed the excellent pH-sensitive behavior of PEG/ poly (acrylic acid-co-N-vinyl pyrrolidone) semi-IPN gel. The conniving behaviour of the semi-IPN can be assigned to the following reason. As an anionic polymer, the semi-IPN contains numerous hydrophilic $-\text{COO}^-$ and $-\text{COOH}$ groups that can convert with each other.

In extreme acid medium (pH 1.7), the $-\text{COO}^-$ groups transformed into $-\text{COOH}$ groups. On the one hand, the hydrogen-bonding interaction among $-\text{COOH}$ groups were the additional physical cross linking; as a result, the electrostatic repulsion among $-\text{COO}^-$ group was restricted, and so the network tends to shrink⁴⁸. As raising external pH, the ratio of $-\text{COO}^-$ groups in polymer network increased and the electrostatic repulsion between the carboxylate groups are more vehemently dominates over the hydrogen bonding interaction between carboxylic acid groups. For assessing the pH reversibility of the swelling–deswelling oscillation behavior was investigated in buffer solution of phosphate between pH 1.7 and 7.8 (Fig. 6b). It can be noticed that the hydrogel exhibited higher swelling capability at pH 7.8, but the swollen gel rapidly shrinks at pH 1.7 and the intriguing on–off switching effect was observed. After three On–Off cycles, the hydrogel still has better sensitivity, signalling that the semi-IPN possess excellent pH reversibility.

3.3. Study of swelling of the hydrogels

Several hydrogels synthesized by varying concentration of monomer (acrylic acid and vinyl pyrrolidone), initiator, crosslinker (MBA) and PEG were used for swelling at different time intervals in double distilled water. The results of swelling viz. equilibrium swelling ratio (ESR) and equilibrium swelling time (t_{eq}) in water for all of these hydrogels are shown in Fig. 7a. From this figure it is observed that both ESR and t_{eq} decreases with increase in initiator concentration. At higher initiator concentration hydrogels of low molecular weight with more chain ends are organized resulting in low ESR and low t_{eq} because of network imperfection in the gel⁴⁹. Similarly, increase in crosslinker concentration results in tighter and denser network of the gel. Consequently, ESR decreases at higher crosslinker concentration while t_{eq} increases

since water molecules take longer time to fill a dense network to reach swelling equilibrium. Similarly, with increase in total monomer concentration, ESR increases while t_{eq} decreases. Based on the swelling results as shown in Fig.7a, the hydrogel synthesized with 20 wt% monomer, 1.0 wt% initiator and 1.0wt% crosslinker was chosen and further filled with 1.0, 2.0, 3.0 and 4.0wt% polyethylene glycol (PEG). The ESR is observed to increase further when the poly(acrylic acid-co-N-vinylpyrrolidone), is filled with PEG. However, above 2.0wt% PEG, the ESR of the composite gel decreases. The PEG contains –OH as pendant group and thus in presence of PEG ESR increases. However, PEG also fills up the network of the gel and above 2.0 wt% PEG, there is a marginal decrease in ESR as observed in Fig.3a. In the composite gel the filled network acquires longer time for penetration of water and hence t_{eq} increases with increase in PEG content. The hydrogel containing 2.0 wt% PEG, 1% MBA, 20% monomer concentration and 0.5% initiator showing the highest ESR was also subjected to swelling at varied pH and this hydrogel is observed to show ESR of 4.3, 18.1 and 25.2 at pH of 1.7, 6.8 and 7.8, respectively. The swelling at low pH is due to the protonation of the carboxylic acid groups of the copolymer phase present in the hydrogel. This ionization causes swelling due to electrostatic repulsion. The carboxyl groups of copolymer segments remain protonated up to its point of zero charge pH which is around 8.0. Similarly, the carboxylic groups (COOH) of the gel ionize at a pH above its pKa value (4.26). Meanwhile, the charge repulsion also results in an increasing of ESR that in our case is correlated to higher concentration COO^- groups, which not only due to the dissociation of carboxylic acid group but also from the reaction of partial hydroxylation of γ -lactam group in the alkaline solutions described as in Scheme 2⁵¹.

3.3.1. Swelling kinetics, diffusion and network parameters

The swelling ratio (SR) of the hydrogels at various time intervals was observed to fit well to the following non linear first order rate Eq.5⁵²

$$SR_t = Q_e(1 - e^{-k_1 t}) \quad (6)$$

Here, k_1 is rate constant and Q_e is ESR of the respective hydrogel. The data fitting were carried out by using Levenberg-Marquardt (L-M) algorithm (Origin-8 software) with adjustment of parameter values viz. rate constant (k_1) and initial rate of swelling (r_0) by iteration using chi square (χ^2) and F values. The trend lines of these non linear fittings for hydrogels synthesized with 1, 2, 3 and 4wt% PEG and designated as PEG1, PEG2, PEG3 and PEG4, respectively, are shown in Fig.7bi. Similar trend lines (not shown) were also obtained for hydrogels synthesized with 0.5, 1, 1.5, 2 and 2.5wt% crosslink (designated as MBA0.5, MBA1, MBA1.5, MBA2, MBA2.5 respectively), 15, 20, 25 and 30wt% monomer in water (designated as AA/NVP15, AA/NVP20, AA/NVP25 and AA/NVP30 respectively). The value of k_1 , experimental and calculated ESR of all of these hydrogels are shown in Table 1. The values of statistical parameters, i.e., r^2 , χ^2 and F are also shown in Table 1. It is observed that ESR of the hydrogels calculated using first order rate Eq.5 closely matches the experimental ESR. The values of regression coefficients (r^2) for all of these fittings are also remarked to be close to unity (0.99006 to 0.99887) while these regressions also show low χ^2 (0.003–0.14), the error value of the respective plots was in 10^{-5} order and desirable high F values (3205–19675). All of these results confirm good fitting of the swelling data to first order rate equation.

The study of diffusion through network of hydrogel is pertinent for its application in drug release. The diffusion in polymer is passive but it can be activated by swelling in release

medium, i.e., water in the present case and also by various external physical forces like polar, osmotic or convective forces⁵³. For understanding the diffusion mechanism, the swelling data were also fitted to the following Eq.6 and Eq.7 to evaluate the diffusion characteristics viz. diffusion constant (k_D), diffusion exponent (n) and diffusion coefficient (D) of the hydrogels.⁵³

$$F = \frac{W_t}{W_e} = k_D t^n \quad (7)$$

$$D = \pi r^2 \left(\frac{k_D}{4} \right)^{\frac{1}{n}} \quad (8)$$

Here F is fractional water uptake and r is radius of cylindrical hydrogel sample. The data fitting and non linear regression was similar to swelling kinetics as shown in inset of Fig.7bi for PEG1, PEG2, PEG3 and PEG4 composite gels. Similar trend lines were obtained for other hydrogels. The values of diffusion characteristics, i.e., k_D , n and D of the hydrogels are also shown in Table 1. From Table 1 it is observed that hydrogels prepared with varied PEG, MBA and monomer concentration shows n values ranging from 0.5 to around 0.7 signifying Non-Fickian anomalous diffusion, i.e., in these cases rate of diffusion and rate of chain relaxation of the gels are comparable. The hydrogels prepared with varied initiator concentrations shows n values close to 0.5 indicating Fickian Case-1 diffusion, i.e., in these cases rate of diffusion is slightly lower than rate of chain relaxation.⁵⁵ The values of statistical parameters, i.e., r^2 , χ^2 and F for these non linear fittings as shown in Table 1 also confirms good fitting of swelling data to diffusion equation.

Several network parameters such as average molecular weight between cross links (M_c), crosslink density (ρ_c) and mesh size (ζ) of the gels were obtained using eq. (4) – (4d) based on experimental swelling data in double distilled water at pH 7.8. The table 1 data

exploits that M_c and ζ decreases whereas ρ_c increases with increase in cross linker concentration from MBA1 to MBA2.5. This observation demonstrated that the number of networks increases in the gel matrix with increase in crosslinker concentration. Molecular weight of the hydrogels decreases with an increment of initiator dose for polymerisation.²⁵ It is also noticed that the M_c and ζ also show the ascending trend with increasing PEG content which corresponds to the formation of more branched multiple side chains in the hydrogel generated during free radical reaction.

3.3.2. Time-dependent swelling behaviours in saline solution

As shown in Fig. 8, the water absorption of the semi-IPN in NaCl, CaCl₂, AlCl₃ and FeCl₃ solutions increased with prolonging contact time, reached a maximum absorption and then decreased with further prolonging contact time until swelling almost disappeared; however, no similar behaviors can be observed in NaCl solution. The unnatural time dependent swelling effect can be attributed to the following reasons. In multi-valence saline solution, Ca²⁺ and Al³⁺ may complex with hydrophilic -COO⁻ groups to form an additional and so the cross linking degree of hydrogel network increased with prolonging the contact time.⁵⁶ As a result, the swollen network gradually collapsed and the initially absorbed water was squeezed out of the network under this action. Because Na⁺ has no complexing action with -COO⁻ groups, there is no time-dependent swelling effect in NaCl solution. The purpose swelling behaviour of the hydrogel in ferric ion simulated liquid is that ferric ion is also a component of human body fluid. Therefore in ferric ion bearing solution the swelling is better with respect to Al³⁺ containing solution. As Al³⁺ is lower in size with respect to Fe³⁺, so it is justified in the data that the complexion ability of Al³⁺ is much prominent than Fe³⁺ ion.

3.4. In vitro drug release study

Similar to swelling ratio, loading and entrapment efficiency of these drugs are also observed to increase with decrease in crosslinker wt%, increase in wt% of PEG and increase in solution pH from 1.7 to 7.8. From the FTIR results it is proved that there is no significant electrostatic interaction between hydrogel and drug molecules. The cumulative release profile of the drug from these hydrogels is presented in Fig.8 and ii for varied crosslinker wt% and PEG wt%, respectively. The release profile of PEG1.0 hydrogel at pH 7.8 and 1.7 is shown in Fig.8. From all of these figures it is observed that an initial burst release of the drug is followed by a sustained rate of release for all of these hydrogels. Initially the fast release rate of drug occurs from the surface of the hydrogel due to high concentration gradient of the drug between the release medium, i.e., water and the surface of the gel.⁵⁷ As the release of the drug continues, its concentration in the release medium increases and hence the concentration gradient of drug between gel and release medium decreases and entrapment of the remaining drug in the gel network slow down further release at low concentration gradient.⁵⁸ Similar release profiles were reported for release of model protein and drug from various IPN type hydrogels.⁵⁹⁻⁶²

Fitting of drug release data to model equations

For evaluating the release kinetics, the first 60% of the drug release data of the hydrogels were fitted to the following i) Donbrow- Samuelov (Donbrow & Samuelov, (1980) zero-order kinetics (Eq.9), ii) Higuchi model (Higuchi, 1963)(Eq.10), and iii) Korsmeyer–Peppas model (Korsmeyer, Gurny, Doelker, Buri & Peppas, 1983) (Eq.11). Similar to swelling kinetics nonlinear Levenberg-Marquardt (L-M) algorithm (Origin-8 software) was also used for these fittings.

i) Zero order Donbrow- Samuelov model $m_{Dt} = m_{De} + K_0t$ (9)

ii) Higuchi model $m_{Dt} = m_{De} + K_H t^{1/2}$ (10)

iii) Korsmeyer–Peppas model $F_D = \frac{m_{Dt}}{m_{De}} = K_{KP} t^n$ (11)

Where m_{Dt} and m_{De} are amount of drug released at time t and infinity (at equilibrium), respectively, K_0 , K_H and K_{KP} are constant of the concerned model corresponding to structural and geometrical character of the dosage form and the diffusion exponent 'n' signifies mechanism of drug release. It is noticed that the values of 'n' ranges from 0.38 to 0.61 which intends diffusion assisted drug release of the hydrogels. The fitting of drug release data to these models stated above are shown in Fig. 9i, ii and iii for Donbrow-Samuelov zero order, Higuchi and Korsmeyer–Peppas models, respectively with PEG1, PEG2, PEG3 and PEG4 hydrogels.^{63,64}

Evaluation of drug action

The chemical activity of the drug was investigated by detecting the UV spectra of pure cefadroxil drug in water and also these drugs released in water from hydrogels at wavelength of 272 nm for cefadroxil as exhibited in Fig.10. The respective spectra appear to be virtually identical proposing that there was no significant change in chemical and bioactivity of the drug during its loading and sustain release. As a matter of fact similar type of comparison to evaluate the chemical and bioactivity of drug has also been reported elsewhere.⁶⁵

Conclusion

Sequential semi-IPN type pH-sensitive phyllosilicate filled polyethylene glycol based composite hydrogel of acrylic acid and N-vinyl pyrrolidoneis constructed here by N,N-methylenebisacrylamide as a gelling agent which results a combination of chemical crosslink

and physical crosslink. The results of 2^4 factorial design which is depicted in sign table, experiment indicated a substantial contribution of all the four main effects of PEG content, crosslinker concentration, initiator concentration and total monomer concentration, on swelling response of the hydrogel. FTIR and DSC measurements testify that the semi-IPN hydrogel is founded on the formation of the hydrogen bond between the carbonyl group in the vinyl pyrrolidone network and the carboxylic acid group on the AA segment as well as the chemical crosslinking through reaction. The semi-IPN hydrogel is non-responsive to ionic strength over the high concentration of inorganic salt are also investigated. In this work it is noticed that clay normally enhances the water uptake amount with desirable strength. Molecular weight between two crosslinks, crosslink density and mesh size of the hydrogels were also assessed. The pH reversibility of the hydrogels increased with increase in PEG wt%. Drug release data is also successfully fitted with the Korsmeyer–Peppas model.

References

1. P. Gupta, K Vermani, S Gary. *Research focus*, 2002; DDT vol. 7: 569. Dagani R. *Chem Eng News* 1997. **75**, 26.
2. J. M. Rosiak, and F Yoshii, *Nucl. Instrum. Methods Phys. Res.*, B 1999, **151**, 56.
3. J.M. Harris, *Poly(ethylene glycol) chemistry: biotechnical and biomedical applications*. 1992, New York: Plenum Press.
4. Shuping Jin, Jianxion Gu, Yujun Shi, Kerang Shao, Xinghai You, and Guoren Yue. *European Polymer Journal* 2013, **49**, 1871.
5. M. T. Razzak, D Darmawan, and Zainuddin Sukirno, *Radiat. Phys. Chem.*, 2001, **62**, 107.
6. Schmidt, Daniel, Deepak Shah, and Emmanuel P. Giannelis, *Current Opinion in Solid State and Materials Science*, 2002, **6**, 205.
7. Kazutoshi Haraguchi, and Tora Takehisa, *Advanced Materials*, 2002, **14**, 1120.
8. Patrick Schexnailder, and Gudrun Schmidt, *Colloid and Polymer Science*, 2009, **287**, 1.
9. Kazutoshi Haraguchi, Toru Takehisa, and Simon Fan, *Macromolecules*, 2002, **35**, 10162.

10. Kazutoshi Haraguchi, Toru Takehisa, and Makiko Ebato, *Biomacromolecules*, 2006, **7**, 3267.
11. Xiang, Yuanqing, Zhiqin Peng, and Dajun Chen, *European Polymer Journal*, 2006, **42**, 2125.
12. Kazutoshi Haraguchi, *Current Opinion in Solid State and Materials Science*, 2007, **11**, 47.
13. S.G. Adoor, M. Sairam, L.S. Manjeshwar, K.V.S.N. Raju, and T.M. Aminabhavi, *J. Membr. Sci.*, 2006, **285**, 182.
14. T. Lundstedt, E. Seifert, L. Abramo, B. Thelin, Å. Nyström, J. Pettersen, and R. Bergman, *Chemometrics and Intelligent Laboratory Systems*, 1998, **42(1)**, 3.
15. I. D. Mall, V. C. Srivastava, G. V. A. Kumar, and I. M. Mishra, *Colloids and Surfaces A: Physicochemical and Engineering Aspects*, 2006, **278**, 175.
16. W. Wang, and A. Wang, *Carbohydrate Polymers*, 2010, **80**, 1028.
17. Xue, Wei, Simon Champ, and Malcolm B. Huglin. *Polymer*, 2001, **42**, 3665.
18. Z.Y. Ding, J.J. Akloins, and R.J. Salovey, *Polymer Science Part B: Physics*, 1991, **29**, 1035.
19. J. Chen, H. Park, and K. Park, *Journal of Biomolecular Materials Research*, 1999, **44** 53.
20. W. Xue, S. Champ, and M.B. Huglin, *Polymer*, 2001, **42**, 3665.
21. T. Canal, and N. A. Peppas, *J Biomed Mater Res.*, 1989, **23(10)**, 1183.
22. E. R. Morris, A. N. Cutler, S. B. Ross-Murphy, D. A. Rees, and J. Price, *Carbohydrate Polymers*, 1981, **1**, 5.
23. Oyama, Hideko Tamaru, Wing T. Tang, and Curtis W. Frank, *Macromolecules*, 1987, **20**, 474.
24. Xingfeng Zhu, Ping Lu, Wei Chen, Jian Dong, *Polymer*, 2010, **51(14)**, 3054.
25. R.S. Tomar, I. Gupta, R. Singhal, and A. K. Nagpal. *Polymer Plastics Technology and Engineering*, 2007, **46**, 481.
26. G. Odian, Radical chain polymerization. In *Principle of polymerization* (3rd ed.,) .1991. pp.198–334,. Singapore: John Wiley & Sons Inc.
27. W. Wang, and A. Wang, *Carbohydrate Polymers*, 2010, **80**, 1028.
28. D.C. Montgomery, 1997. *Design and Analysis of Experiments*, 4th ed. Wiley, New York, pp. 290–341.
29. Lundstedt, Torbjörn, Elisabeth Seifert, Lisbeth Abramo Bernt Thelin, Åsa Nyström, Jarle Pettersen, Rolf Bergman., *Chemometrics and Intelligent Laboratory Systems*, 1998, **42.1**, 3.
30. C. Damm, M. R. Mallembakam, A. Voronov, W. Peukert, *J Appl. Polym. Sci.*, 2011, **120**, 799.
31. A. Li, and A. Wang, *European Polymer Journal*, 2005, **41**, 1630.
32. S. Nagarajan, K. Sabdham, V. Srinivasan, *Macromolecular Materials and Engineering*. 1997, **245**, 9.

33. L. Zheng, S. Xu, Y. Peng, J. Wang, G. Peng, *Polymer For Advance Technol.*, 2007, **18**, 194.
34. K. Xu, J. Wang, S. Xiang, Q. Chen, W. Zhang, P. Wang, *Applied Clay Sci.*, 2007, **38**, 139.
35. Q. Tang, J. Wu, H. Sun, S. Fan, D. Hu, Jianming Lin, *Polym. Composites.*, 2009, **30**, 1183.
36. A. J. Marshall J. Blyth, C. A. B. Davidson, *C. R. Lowe Anal. Chem.*, 2003, **75**, 4423.
37. Jin, Shuping, Jianxiong Gu, Yujun Shi, Kerang Shao, Xinghai Yu, and Guoren Yue, *European Polymer Journal*, 2013, **49**, 1871.
38. J. F. Yaung and T. K. Kwei, *J. Appl. Polym. Sci.*, 1998, **69**, 921.
39. D. M. Devine and C. L. Higginbotham, *European Polymer Journal*, 2005, **41**, 1272.
40. D. M. Devine and C. L. Higginbotham, *Polymer*, 2003, **44**, 7851.
41. P. Bures, and N. A. Peppas, *ACS Polym. Mater. Sci. Eng.*, 2000, **83**, 506.
42. El-Badry, Mahmoud, Gihan Fetih, and Mohamed Fathy. *Saudi Pharmaceutical Journal*, 2009, **17**, 217.
43. Huang, Zhanhua, Shouxin Liu, Bin Zhang, Lili Xu, Xiaofeng Hu. *Carbohydrate Polymers*, 2012, **88**, 609.
44. D. Shanmukaraj, and R. Murugan, *J. Power Sour.*, 2005, **149**, 90.
45. Mahmoud A. Hussein, Baha M. Abu-Zied, and Abdullah M. Asiri, *Polym. Compos.*, 2014, **35**, 1160, doi: 10.1002/pc.22763.
46. MH Cohen, and D. Turnbull, *J. Chem. Phys.*, 1959, **31**, 1164.
47. Shu-Guang Wang, Xue-Fei Sun, Xian-Wei Liu, Wen-Xin Gong, Bao-Yu Gao, Nan Bao, *Chemical Engineering Journal*, 2008, **142**, 239.
48. Kim, Sang-Gyun, Gyun-Taek Lim, Jonggeon Jegal, Kew-Ho Lee, *Journal of Membrane Science*, 2000, **174**, 1.
49. Wang, Wenbo, and Aiqin Wang, *Carbohydrate Polymers*, 2010, **80**, 1028.
50. Shen, Liang-liang, Gui-xia Liu and Yun Tang, *Acta Pharmacol Sin*, 2007, **28**, 2053.
51. S. Jin, M. Liu, F. Zhang, S. Chen, and A. Niu, *Polymer*, 2006, **47(5)**, 1526.
52. S. Li, R. Vatanparast, and H. Lemmetyinen, *Polymer*, 2000, **41(15)**, 5571.
53. Z. Seden Akdemir, and Apohan Nilhan Kayaman, *Polymers for Advanced Technologies*, 2007, **18**, 932.
54. Y.M.P.S. Mohan, K.K. Murthy, M. Raju, *Reactive & Functional Polymers*, 2005, **63**, 11.
55. S. Lj Tomić, M.M. Mičić, J.M. Filipović, and E.H. Suljovrujić, *Radiation Physics and Chemistry*, 2007, **76**, 801.
56. S. B. Hua, and A. Q. Wang, *Carbohydrate Polymers*, 2009, **75**, 79.
57. Nitin S. Patil, Jonathan S. Dordick, and David G. Rethwisch, *Biomaterials*, 1996, **17**, 2343.
58. K. S. V Krishna Rao, B. Vijaya Kumar Naidu, M.C.S. Subha, M. Sairam, and T.M. Aminabhavi, *Carbohydrate Polymers*, 2006, **66**, 333.

59. Pietro Matricardi, C. Di Meo, T. Coviello, W. E. Hennink, and F. Alhaique, *Advanced Drug Delivery Reviews*, 2013, **65**,1172.
60. Nitin S. Patil, Jonathan S. Dordick, and G. Rethwisch David. "*Biomaterials*, 1996, **1724** 2343.
61. Raghavendra V Kulkarni, V Sreedhar, S. Mutalik, C. M. Setty, and B. Sa, *International Journal of Biological Macromolecules*, 2010, **47**, 520.
62. Raghavendra V. Kulkarni, R. Boppana, Mohan G Krishna, S Mutalik, and N. V. Kalyane, *Journal of Colloid and Interface Science*, 2012, **367**, 509.
63. 62. R. V. Kulkarni, V. Sreedhar, S. Mutalik, C. M. Setty, and B. Sa, *International Journal of Biological Macromolecules*, 2010, **47**, 520.
64. R. W. Korsmeyer, R. Gurny, E. Doelkar, P. Buri, and N. A. Peppas,. *International Journal of Pharmaceutics*, 1983, **15**, 23.
65. Chouhan, Raje, and Anil K. Bajpai. "Release dynamics of ciprofloxacin from swellable nanocarriers of poly (2-hydroxyethyl methacrylate): an in vitro study." *Nanomedicine: Nanotechnology, Biology and Medicine*, 2010, **6(3)**, 453.

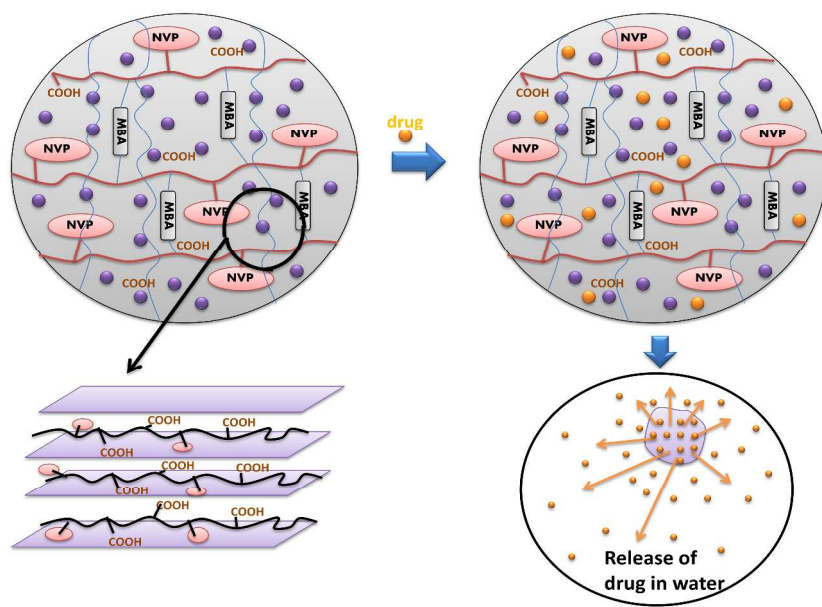


Fig. abstract

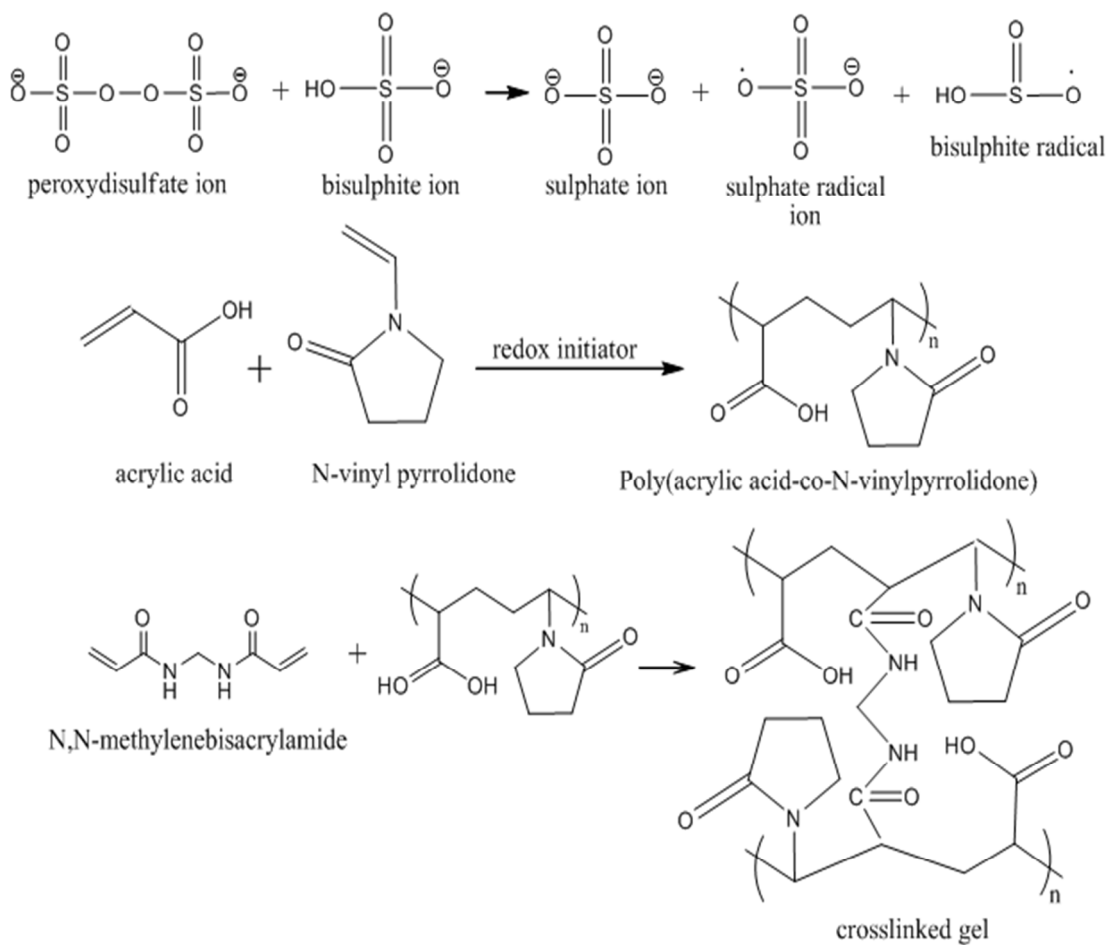
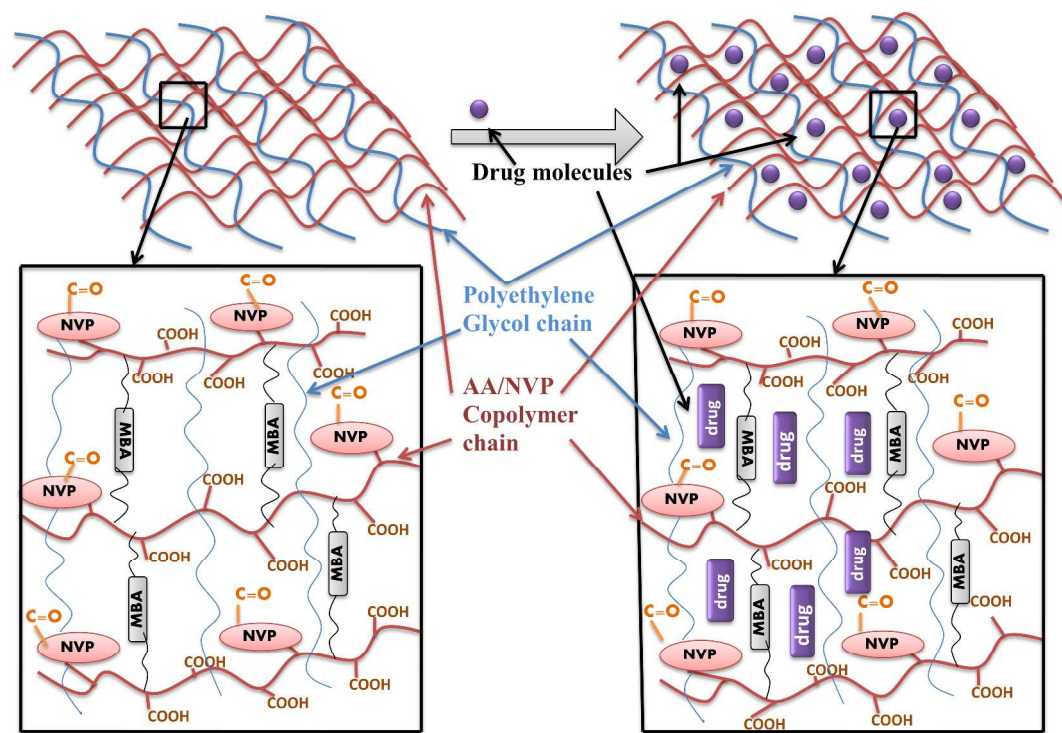
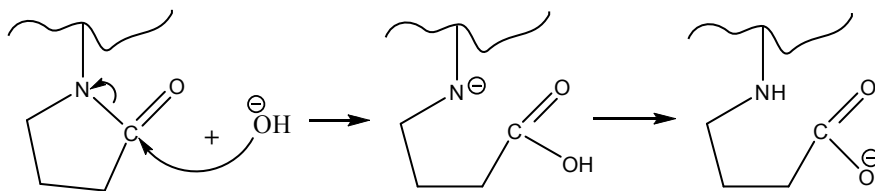


Fig.1a Formation of semi-IPN and its plausible interaction with drug



Scheme 1 : Formation of compsite hydrogel



Scheme 2: partial hydrolization of N-vinylpyrrolidone

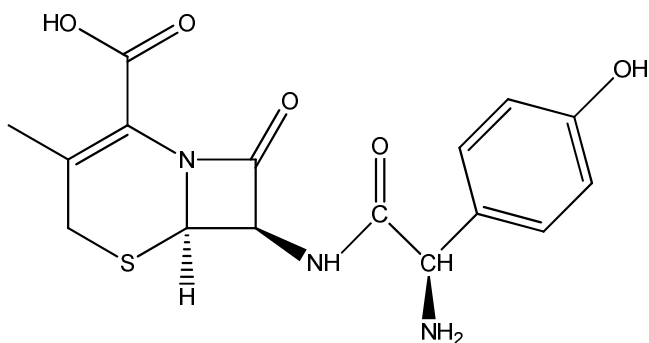


Fig.1b. Chemical structure of cefadroxil

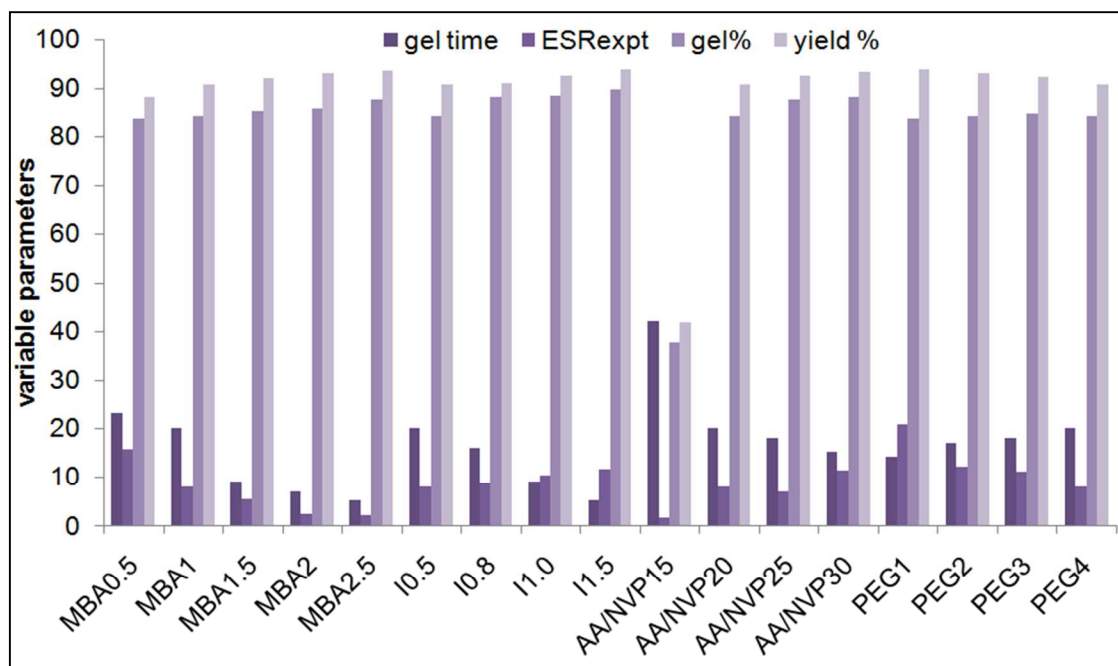


Fig. 1c Effect of initiator (I), monomer (M), crosslinker (MBA) and polyethylene glycol (PEG) on yield or gel% and gel time (Tgel)

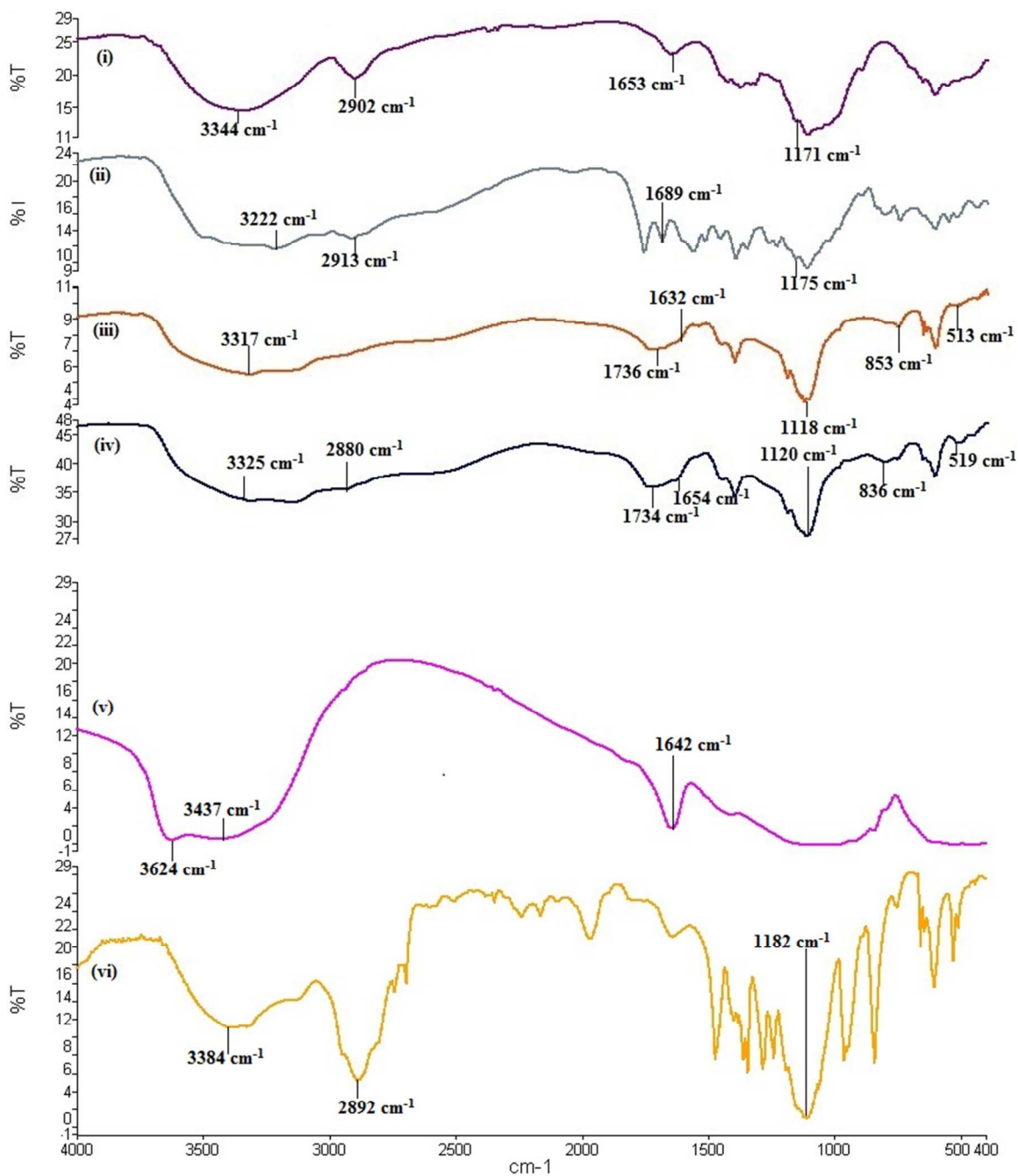


Fig.2 FTIR of the polymer, i. drug loaded gel, ii. cefadroxil, iii. Filler loaded gel, iv. Pure gel, v. filler, vi. PEG

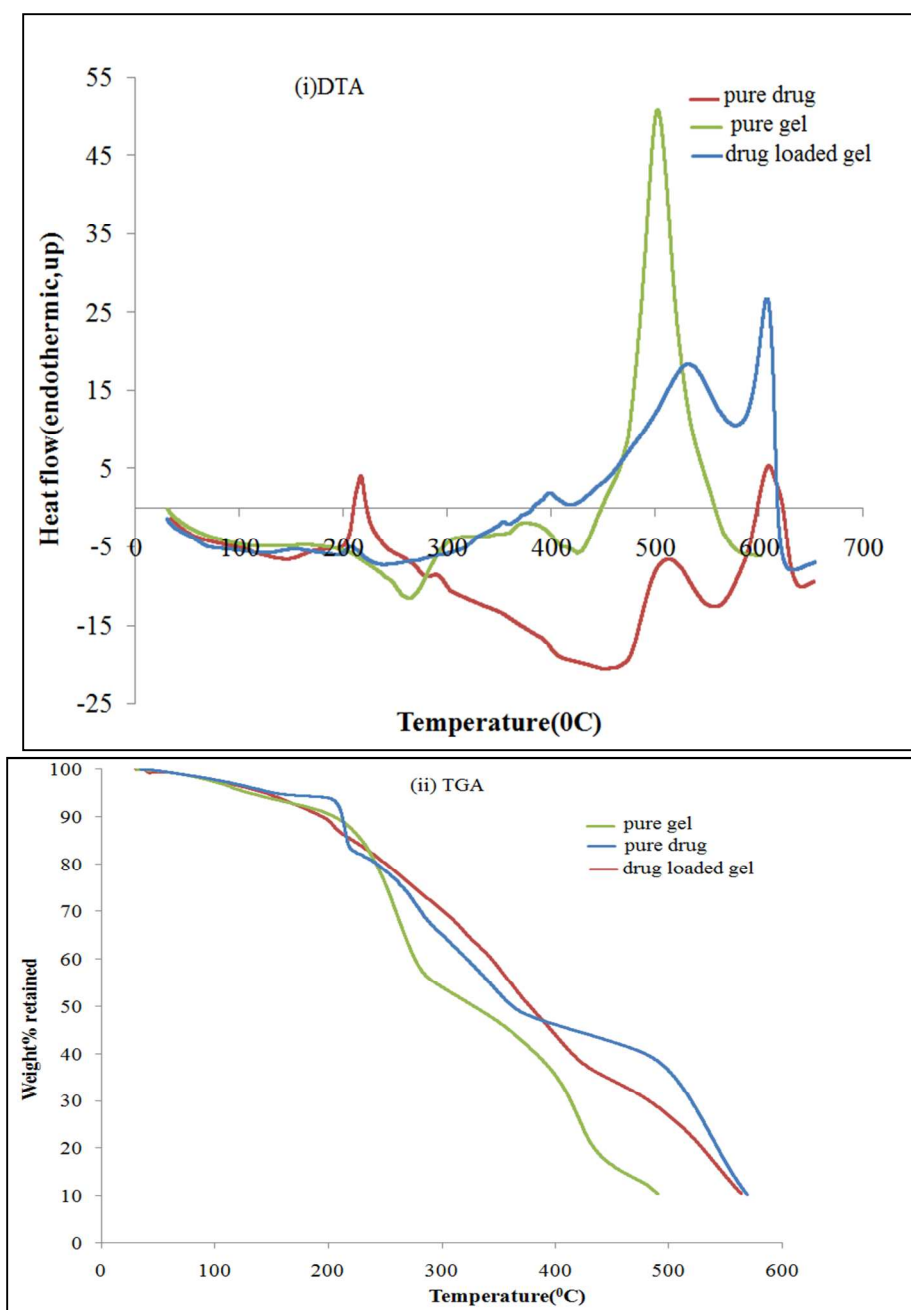


Fig. 3 (i) DTA and (ii) TGA of the polymer

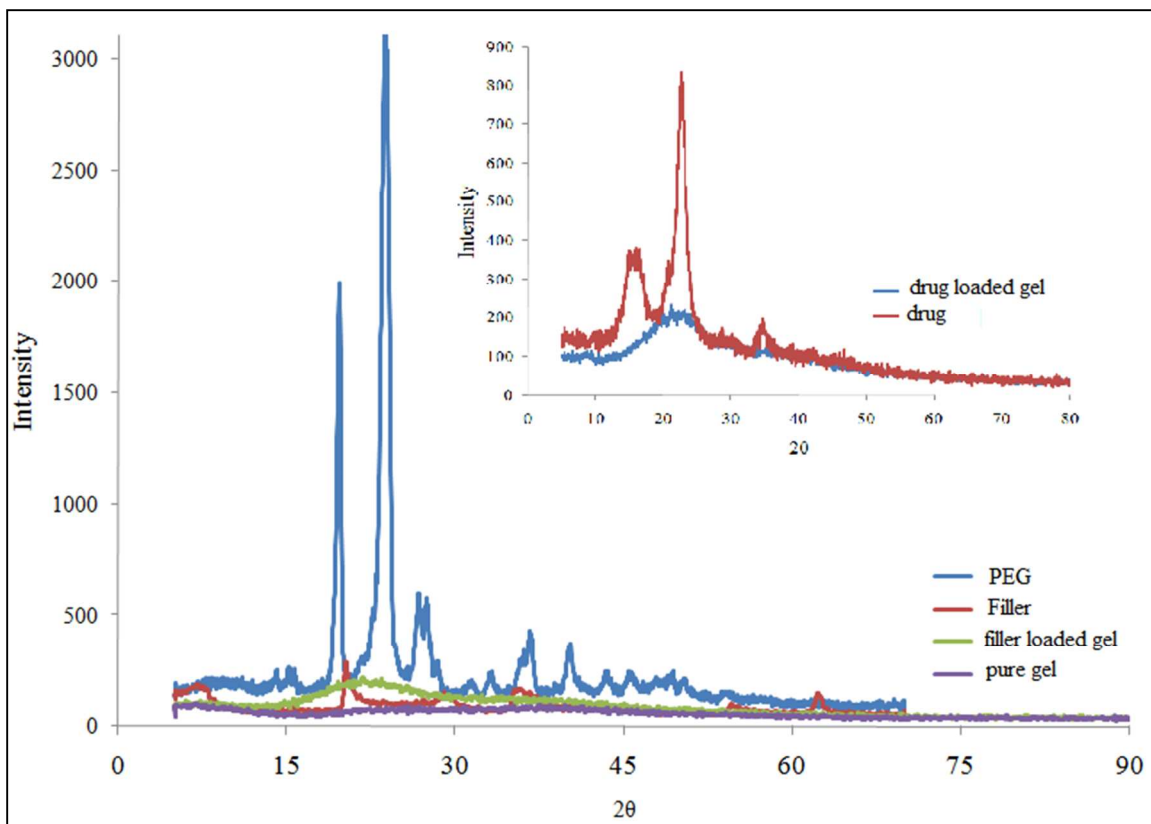


Fig.4 XRD of the polymer and drug

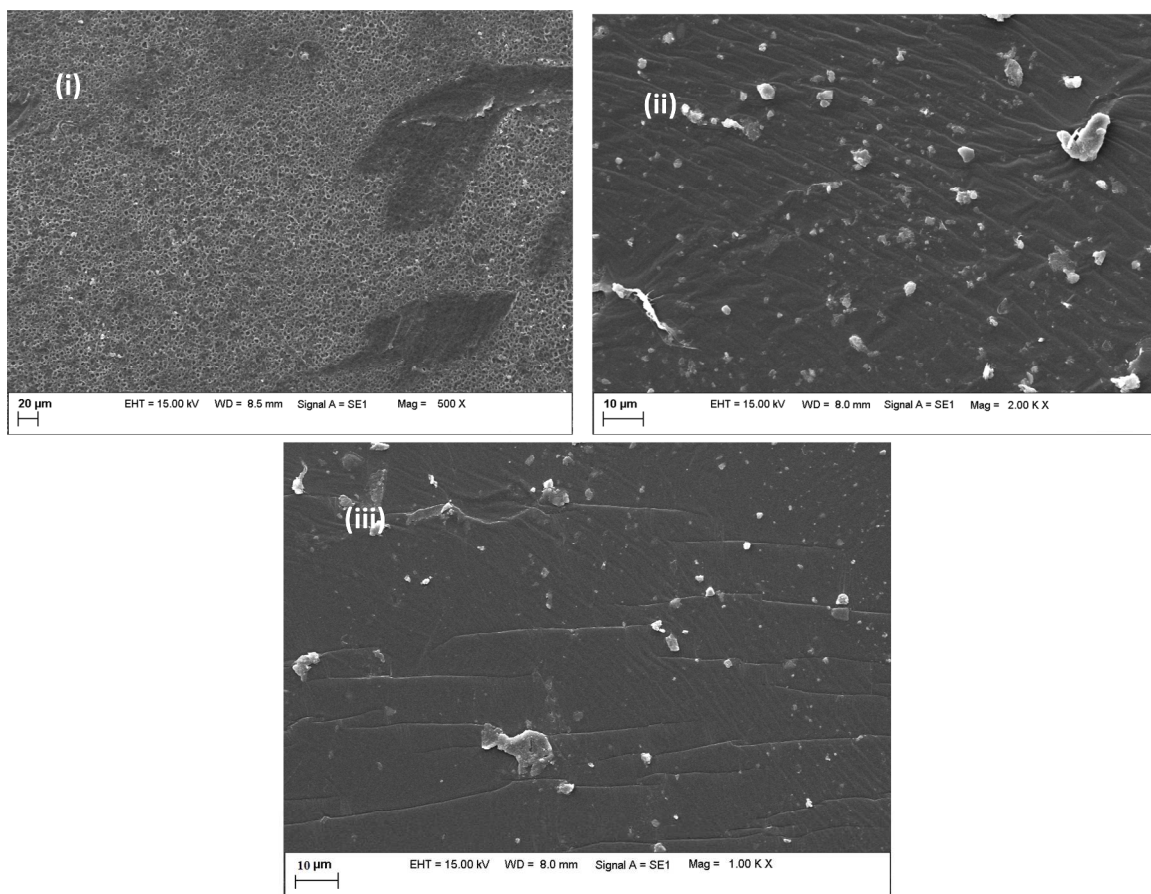


Fig. 5 Scanning Electron Microscope pictures of (i) unfilled gel (ii) clay loaded gel (iii) drug loaded gel.

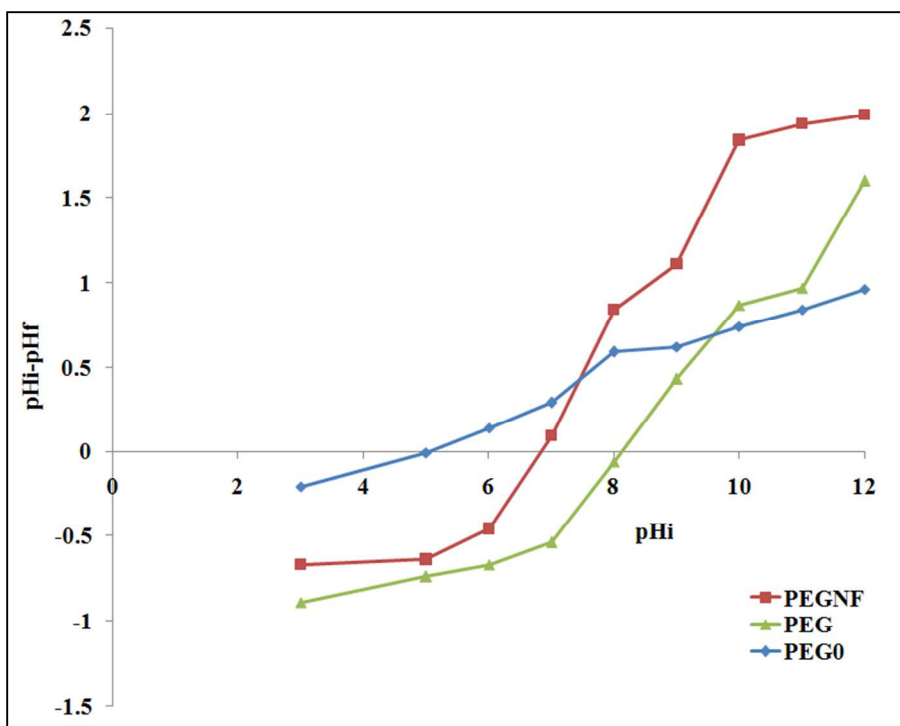


Fig. 6a PZC of filler loaded gel, pure gel and gel without PEG.

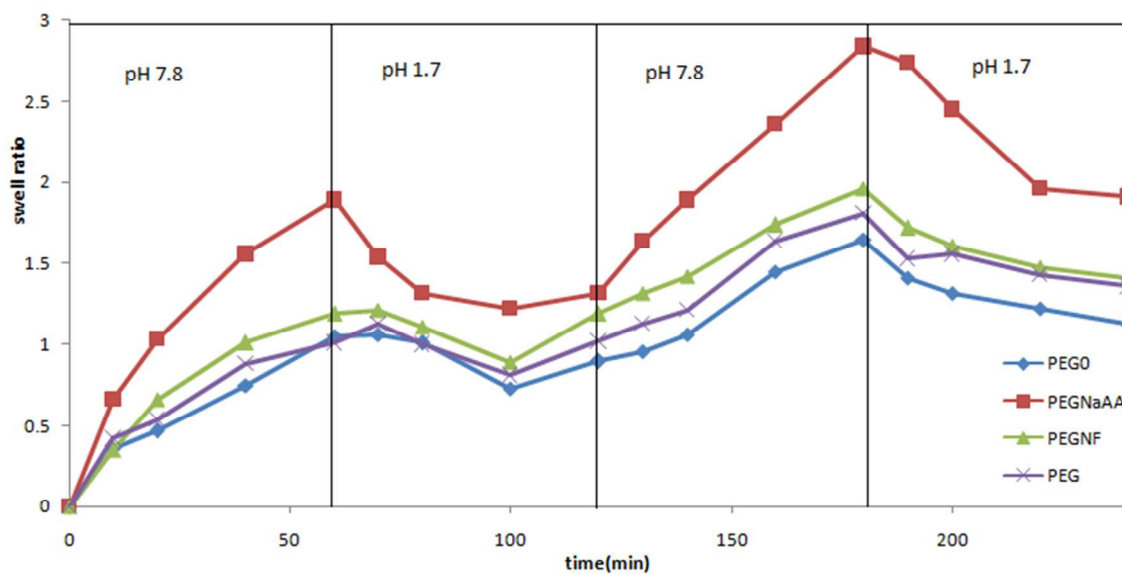


Fig. 6b pH reversibility (switch on-off behavior) of the gels

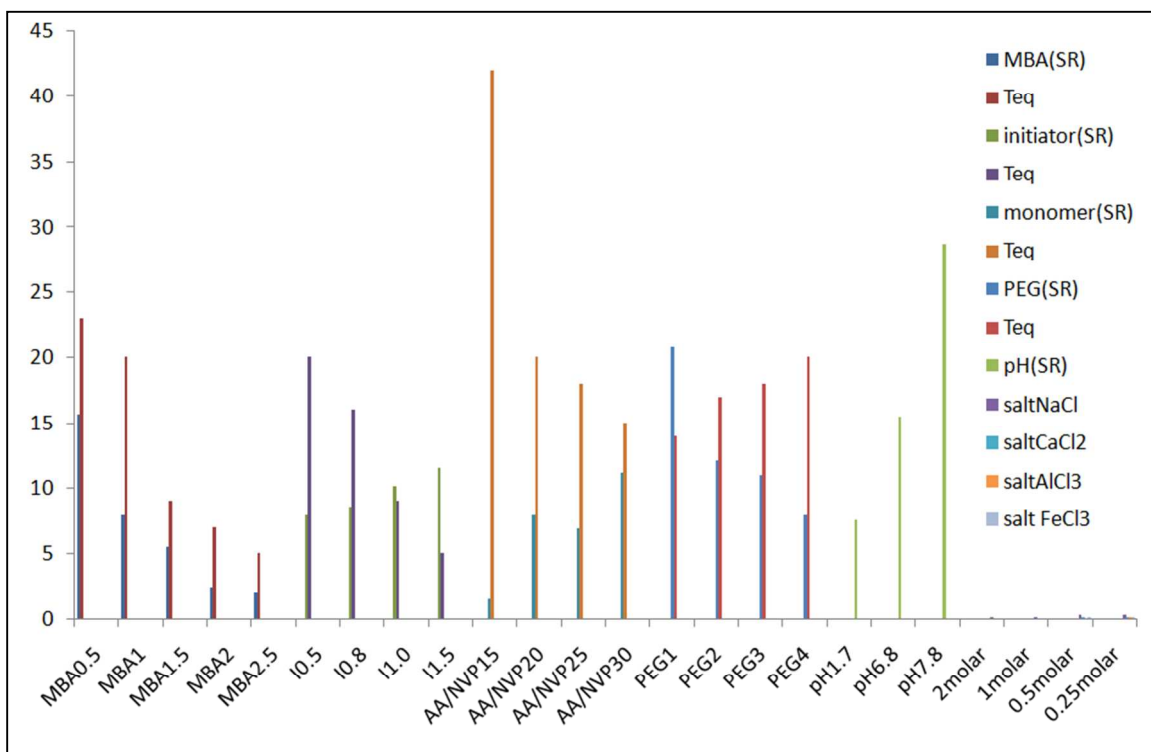
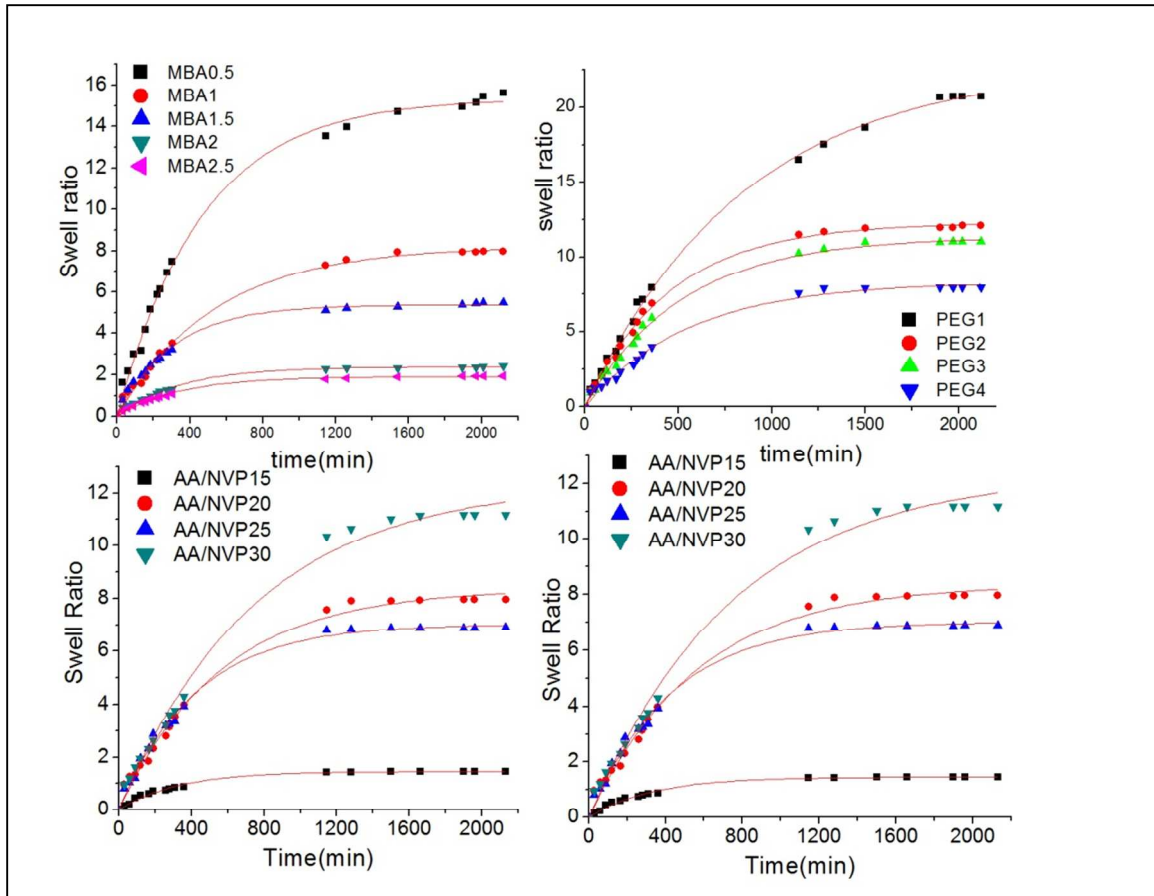


Fig.7a Effect of conc. of initiator, total monomer, crosslinker, PEG, salt and pH on equilibrium swelling ratio.



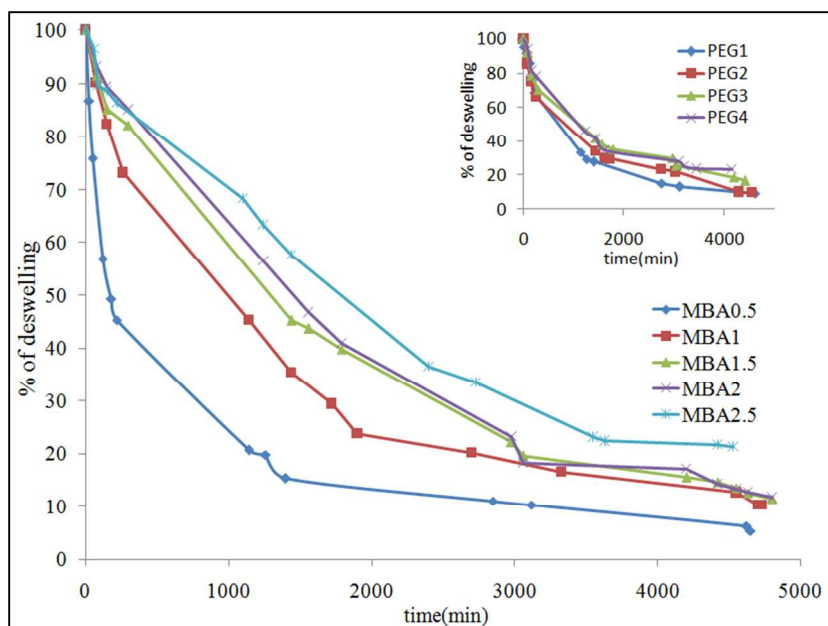


Fig. 7b (i) Non linear fitting of swelling data to 1st order rate equation and diffusion characteristics (ii) Deswelling of the hydrogel at crosslinker (MBA) wt% and varied PEG nwt% (inset)

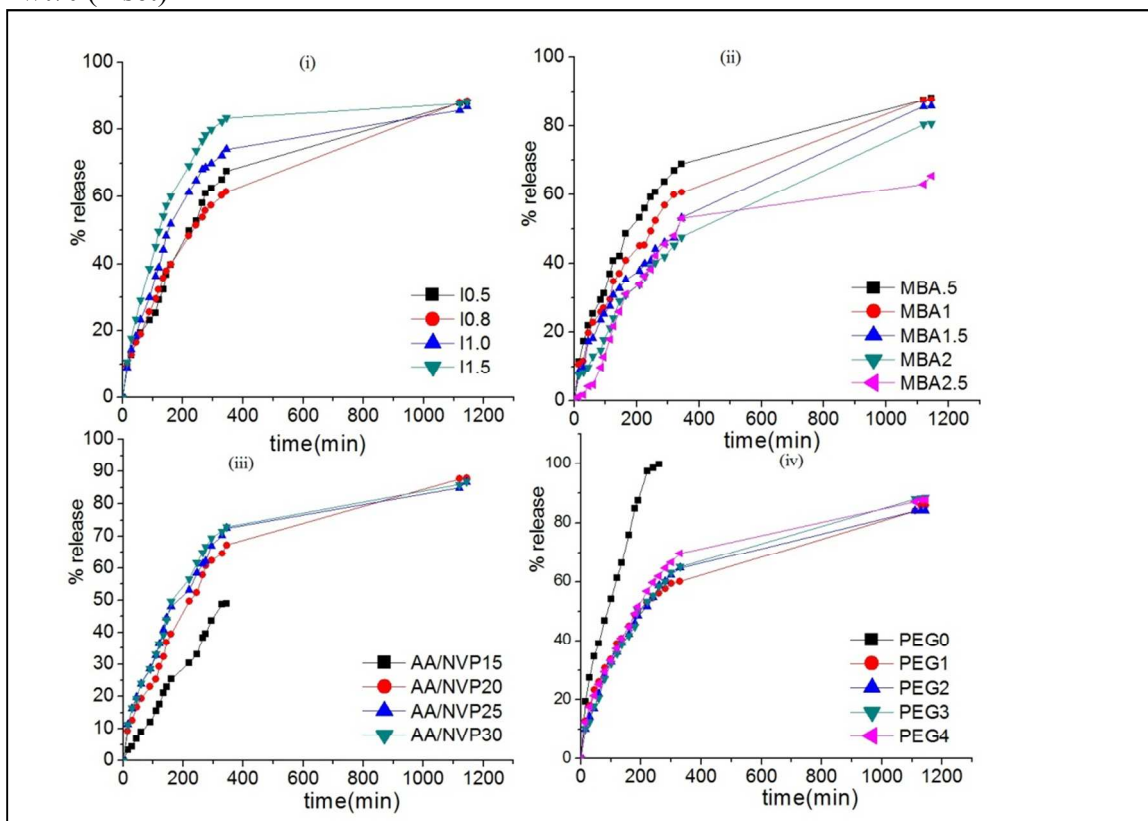
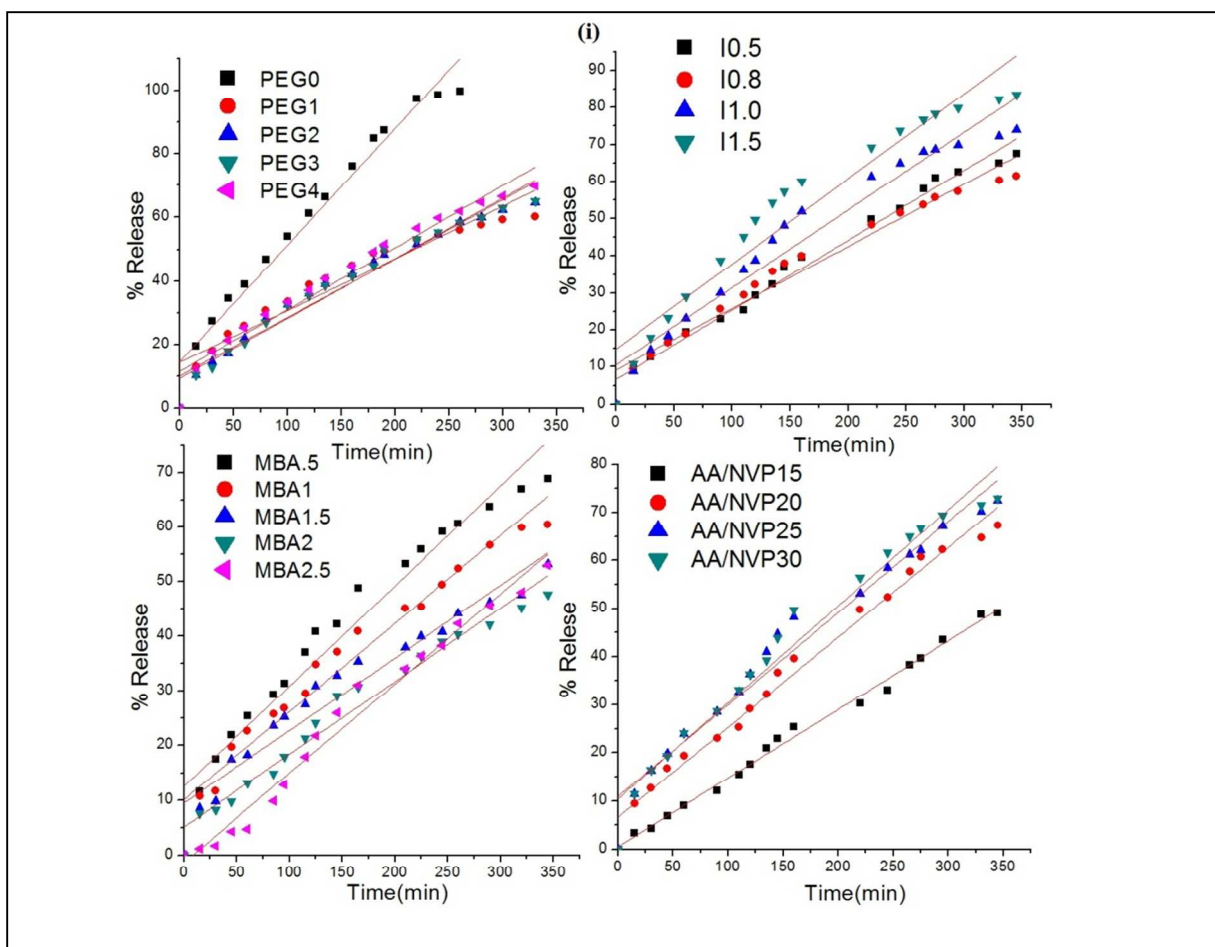
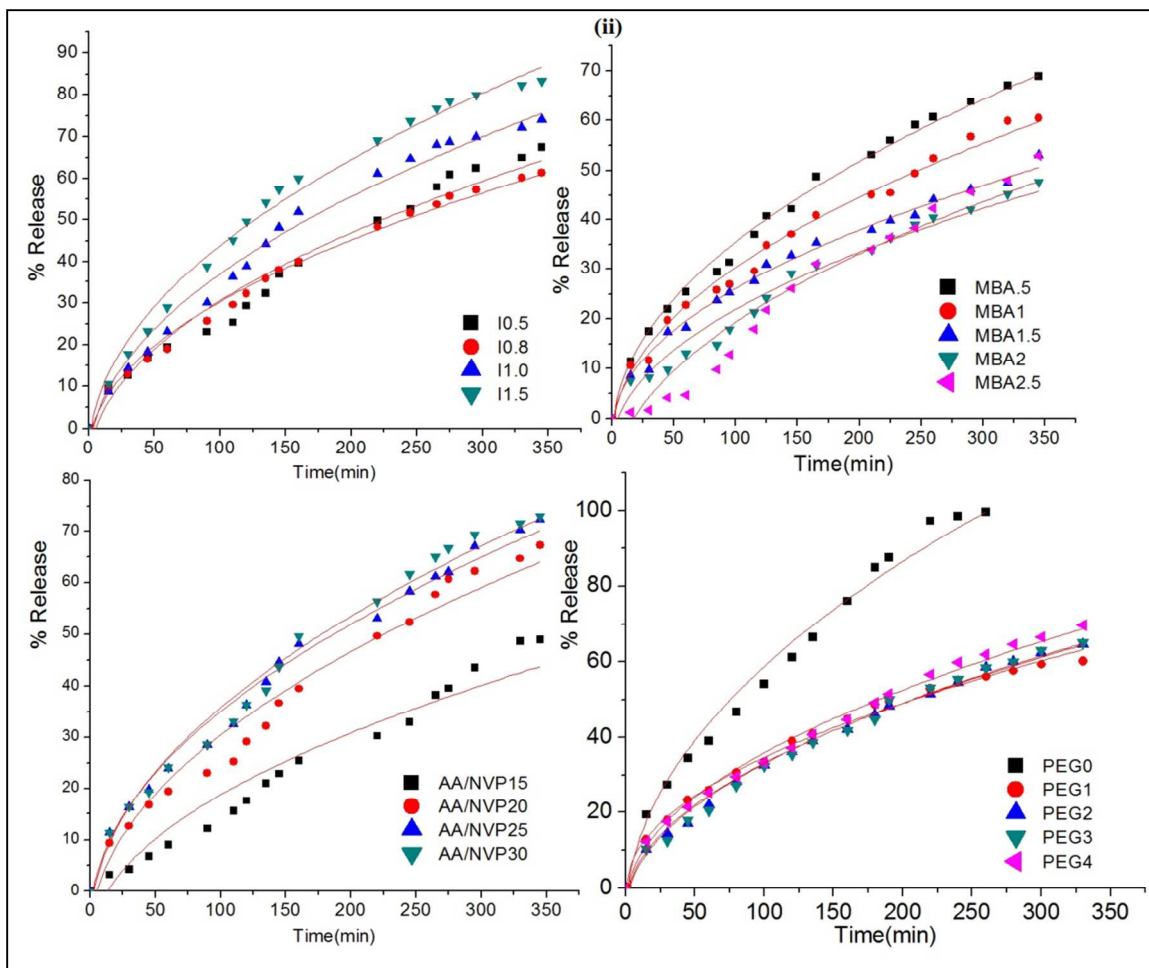


Fig.8 Cumulative release% of cefadroxil drug at i) Initiator wt% , ii) MBA wt%, iii) monomer (acrylic acid and NVP) wt% and iv) PEG wt%





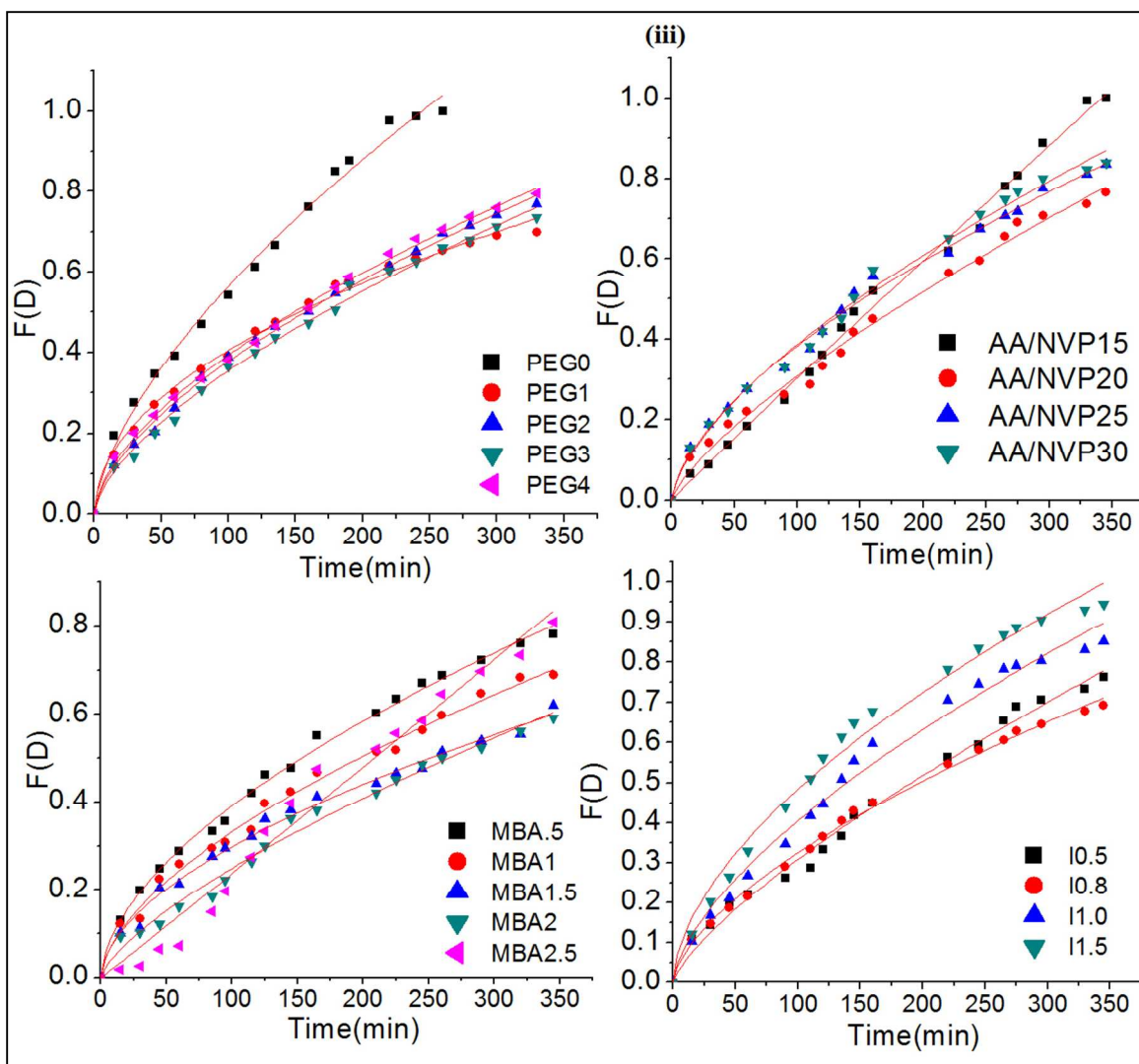


Fig.9 Fitting of drug release data of cefadroxil to (i) Donbrow-Samuelov zero order (ii) Higuchi and (iii) Korsmeier–Peppas model for hydrogels

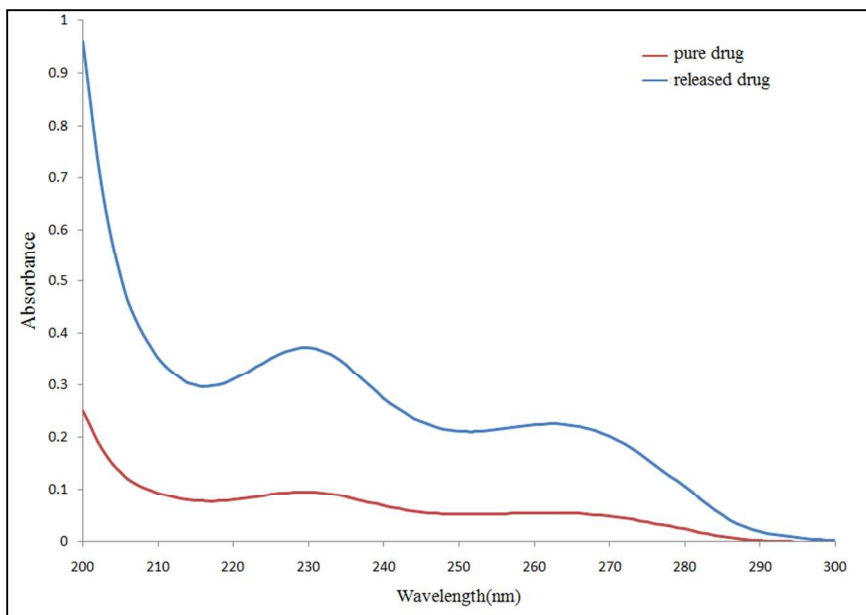


Fig. 10 UV spectra of pure drug and released drug from the hydrogel

Table 1

Swelling diffusion and network parameters of the hydrogels

Polymer code	$K_1 \times 10^2$	$ESR_{\text{expt}}/ESR_{\text{cal}}$ (g/g)	$r^2/\chi^2/F$ value	$K_D/n/D \times 10^6$	$M_c \times 10 / \rho_c \times 10^{-22} / \zeta$
MBA0.5	0.213	15.64/15.36	0.99628/0.11884/7482	0.0283/0.47134/3.44	2.19/3.22/1.58
MBA1	0.186	7.96/8.23	0.99586/0.03817/6296	0.02301/0.50299/4.41	1.57/4.31/1.32
MBA1.5	0.326	5.49/5.39	0.99317/0.02324/5465	0.06789/0.35822/1.43	1.73/4.64/1.38
MBA2	0.294	2.401/2.37	0.99104/0.00607/3920	0.0578/0.37974/1.79	9.93/9.07/1.03
MBA2.5	0.296	1.94/1.91	0.99263/0.00324/4769	0.05722/0.38088/1.79	5.99/1.53/0.79
I0.5	0.186	7.96/8.23	0.99586/0.03817/6296	0.02301/0.50299/4.14	1.1/7.9/1.22
I0.8	0.294	8.59/5.57	0.99527/0.04258/7296	0.05678/0.38353/1.91	2.62/3.33/1.94
I1	0.303	10.16/10.155	0.99491/0.06461/6840	0.05993/0.37631/1.78	1.32/6.19/1.34
I1.5	0.279	11.56/11.54	0.99039/0.15552/3562	0.05318/0.39148/2.02	1.42/5.19/1.41
PEG1	0.117	20.75/22.82	0.99887/0.07342/19695	0.00958/0.61495/6.87	4.79/1.51/8.92
PEG2	0.217	12.103/12.29	0.99758/0.05029/11684	0.03196/0.45992/3.46	1.80/4.49/1.41
PEG3	0.192	11.02/11.36	0.99745/0.04546/10462	0.02525/0.49125/4.17	2.81/3.21/1.77
PEG4	0.180	7.96/8.23	0.99241/0.07082/3500	0.02376/0.49972/4.41	2.10/4.42/1.50
TMC15	0.308	1.458/1.46	0.99006/0.00257/3675	0.06653/0.36378/1.61	2.17/3.67/1.55
TMC20	0.180	7.96/8.23	0.99241/0.00257/3500	0.02376/0.49972/4.41	1.60/5.33/1.31
TMC25	0.238	6.89/7.006	0.99482/0.03338/5937	0.04104/0.42775/2.81	1.13/7.90/1.09
TMC30	0.134	11.172/11.53	0.99273/0.14295/3205	0.01281/0.58084/6.37	1.52/5.97/1.27

K_1 (g gel/g water. minute⁻¹), k_D (s⁻¹), n (-), D (cm²/s), ζ (Å)

Table 2

A design matrix and results of the 2⁴ full factorial experiment on swelling optimization study

Formulation code	Independent variable				Independent variables				Swelling Ratio
	X_1	X_2	X_3	X_4	PEG%	MBA%	Initiator%	TMC%	
F1	-	-	-	-	4	1	0.5	20	7.96
F2	-	-	-	+	4	1	0.5	30	15.64
F3	-	-	+	-	4	1	1.5	20	11.172
F4	-	+	-	-	4	2	0.5	20	10.16
F5	+	-	-	-	1	1	0.5	20	12.103
F6	-	-	+	+	4	1	1.5	30	16.20
F7	-	+	-	+	4	2	0.5	30	12.64
F8	+	-	-	+	1	1	0.5	30	13.5
F9	-	+	+	-	1	1	1.5	20	11.15
F10	+	-	+	-	1	2	0.5	20	19.54
F11	+	+	-	-	4	2	1.5	30	26.112
F12	-	+	+	+	1	1	1.5	30	16.59
F13	+	-	+	+	1	2	0.5	30	21.54
F14	+	+	-	+	1	2	1.5	30	23.75
F15	+	+	+	-	1	2	1.5	20	24.19
F16	+	+	+	+	1	2	1.5	30	24.95

(-) and (+) sign indicate low and high levels of a factor, respectively.